Document Room, DOCUMENT ROOM 36-412
Research Laboratory of Electronics
Massachusetts Institute of Technology

#2

294

NOISE IN ELECTRON BEAMS

CHARLES FRIED

LOAN COPY

TECHNICAL REPORT 294

MAY 2, 1955

RESEARCH LABORATORY OF ELECTRONICS
MASSACHUSETTS INSTITUTE OF TECHNOLOGY
CAMBRIDGE, MASSACHUSETTS

The Research Laboratory of Electronics is an interdepartmental laboratory of the Department of Electrical Engineering and the Department of Physics.

The research reported in this document was made possible in part by support extended the Massachusetts Institute of Technology, Research Laboratory of Electronics, jointly by the Army (Signal Corps), the Navy (Office of Naval Research), and the Air Force (Office of Scientific Research, Air Research and Development Command), under Signal Corps Contract DA36-039 sc-42607, Project 102B; Department of the Army Project 3-99-10-022.

MASSACHUSETTS INSTITUTE OF TECHNOLGY
RESEARCH LABORATORY OF ELECTRONICS

Technical Report 294 May 2, 1955

NOISE IN ELECTRON BEAMS

Charles Fried

This report is based on a thesis submitted to the Department of Electrical Engineering, M.I.T., 1954, in partial fulfillment of the requirements for the degree of Master of Science.

Abstract

This report contains an experimental investigation of beam and noise behavior in various types of electron streams. A continuous, reliable, and semi-automatic measuring technique and apparatus are described. Steady-flow and pulsed operating conditions are applied to convergent- and confined-flow guns. An extensive investigation of beam contour, noise-standing-wave pattern, growing noise wave, and beam instability is presented. The effects of magnetic field, ion neutralization, and interception current are measured over considerable operating ranges. Observations with respect to varying cathode temperatures and results of using cathodes of different type, activity, and quality are included. A low-noise, three-region gun is measured under steady-flow conditions. The transformation of the noise-standing-wave pattern by the accelerating anodes is demonstrated. The constancy of the average of the rms noise-current standing wave is verified experimentally.

I. INTRODUCTION

1.1 JUSTIFICATION FOR CONTINUED STUDY OF THE PROBLEM

A fundamental application of vacuum tubes is the amplifying of small signals. The weakest signal that can still be detected by an amplifier is limited by the noise appearing at the output.

There are two major sources of noise in vacuum tubes. The randomness in the density and velocity of the emitted electrons causes random currents and voltages to appear at the output. This random fluctuation is called shot noise. The other principal type of noise appears in multielectrode tubes. Since the cathode current divides in a random manner among the electrodes, the random interception of current increases the noise content of the beam. This type of noise is known as partition noise.

In longitudinal beam tubes the electrons are usually accelerated in the gun region and then continue to move with an essentially constant velocity in the drift space. The electrons generally form a high-current-density, well-defined beam. From the noise point of view, there is no single theory which can account for all the physical aspects of the problem, but there are various approximate calculations that predict the noise behavior with reasonable accuracy. The usual approach is to seek solutions separately in the different regions of the electron flow and then apply the right initial and boundary conditions, or at least useful approximations thereof.

The solutions for the lowest mode of a finite beam, with an axial magnetic field in the drift space, predicted an infinite noise-current standing wave. The experiments of Cutler and Quate (10), Peter (23), Rowe (19), and Muehe (1) verified the theoretical prediction to a certain degree. The measured standing-wave ratios, however, never exceeded 15 db. Rowe (19) analyzed the effect of the finite cavity gap, partition current, and, in particular, the contributions of higher-order modes to the standing-wave ratio. These calculations agreed fairly well with measured results. Serious discrepancies arose, however: the calculated first minimum was exceedingly deep; the calculated noise maxima for a confined-flow beam were greater than those of the convergent one, although Muehe's experiments indicated that the reverse was true; the calculated space phase of the standing-wave pattern did not agree with the measured values.

In addition to a standing-wave pattern of noise, the measurements of Rowe and Peter indicated the existence of a superimposed "growing noise wave" in an electron beam under certain conditions. There was no satisfactory explanation of the cause and mechanism of this phenomenon. However, it was suggested that the ions in the beam excited the growing wave. The fact that ions were trapped in the beam was proved both theoretically and experimentally by Spangenberg, Field, and Helm (4) and by Muehe (1).

Clearly, discrepancies and unexplained phenomena still exist in electron-beam noise investigations. To reduce the noise figure of traveling-wave tubes, it is important to determine more accurately the factors governing the behavior of noise. The investigations described in the next few sections were undertaken in the hope of shedding more

light on the problem of noise in electron beams.

1.2 THE SCOPE AND OUTLINE OF THE REPORT

The immediate purpose of this report is the extensive experimental determination of the behavior of noise in various types of electron beams. These investigations also include the effects of various parameters and operating conditions on the noise characteristics in each type of electron flow. Another objective of these measurements is to facilitate the thorough checking of existing theories and provide the groundwork for improvement. Within the scope of this report, however, little effort is made toward theoretical implementation.

Since the emphasis is put on experimental data, Section II is devoted to experimental apparatus and techniques. It also includes a brief résumé on ion generation because the degree of beam neutralization is dealt with later as one of the parameters that affect noise behavior. Sections III and IV describe the results of measurements on convergent- and confined-flow beams, respectively. The noise characteristics of impregnated Philips cathodes are compared to those of oxide-coated cathodes. Section V deals with measurements on a low-noise, three-region gun developed by Peter. Section VI describes experiments designed to explore the effect of interception current on beam noise. Finally, Section VII summarizes the most important results and conclusions derived from these investigations.

II. DESCRIPTION OF APPARATUS

2.1 INTRODUCTION

The problems which arose in the experimental study of noise were threefold. The fundamental task was the production of well-defined, long electron beams. A demountable vacuum-tube system was used to generate the various types of electron beams to be investigated. Next, it was necessary to provide equipment for the modulation of the beam and for the measurement of the noise. This apparatus was external to the vacuum-tube system. In addition to the equipment requirements, a certain experimental technique was indispensable both in producing the beam and in making reproducible measurements.

2.2 THE DEMOUNTABLE VACUUM-TUBE SYSTEM

The essential features of the demountable tube proper are shown schematically in Fig. 1. A Pierce gun produced an electron beam which drifted thereafter inside a drift tube. The drift tube was approximately 16 inches long and 2.25 inches in diameter. After leaving the anode, the dc velocity of the electrons did not change until they hit the collector. An axial magnetic field prevented the beam from spreading inside the drift space. A uniformly wound solenoid produced this magnetic field. The field strength was continuously variable from 0 gauss to 850 gauss. The end plates of the drift tube

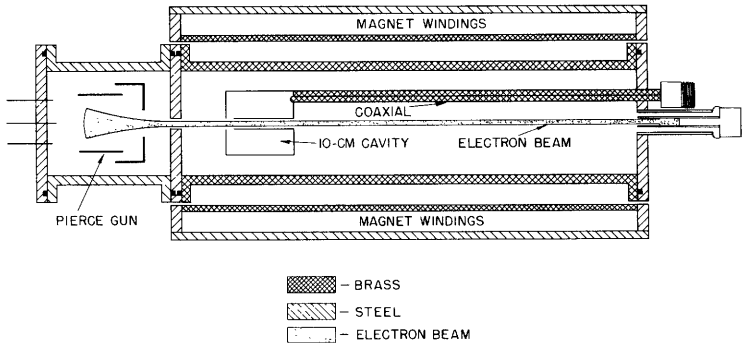

Fig. 1. Electron-beam noise tester.

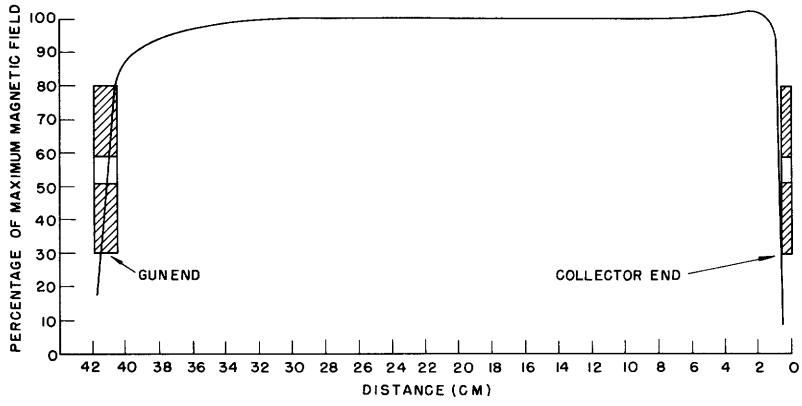

Fig. 2. Magnet calibration: N = 1405 turns; H = 43 gauss/amp.

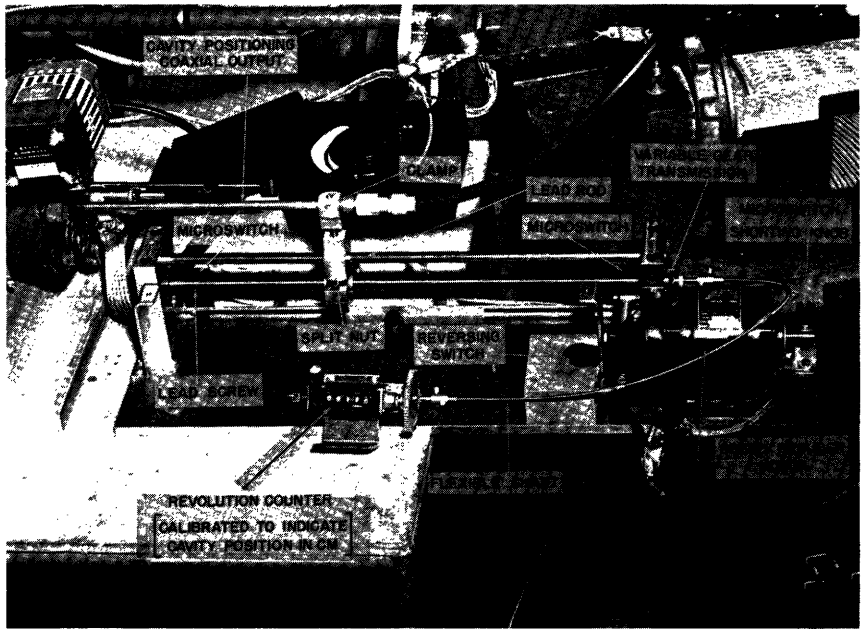

Fig. 3. Automatic cavity-moving mechanism.

and the outer shell of the magnet consisted of cold rolled steel, and these, together with the drift space between the end plates, constituted a closed magnetic circuit. The inner shell of the magnet, the drift-tube walls and all structures within the drift space were made of nonmagnetic materials. The use of nonmagnetic materials and the precise winding of the solenoid were necessary to avoid distortions in the otherwise homogeneous magnetic field. As Fig. 2 shows, the resulting magnetic field attained its final value very rapidly and did not exhibit any appreciable variations along the drift space. Radially directed adjustment screws facilitated the lateral movement of the drift tube. The tube had to be positioned carefully for optimum beam transmission.

Both convergent- and confined-flow electron beams were investigated during the experiments. The latter were produced by parallel Pierce guns immersed in the magnetic field inside the drift tube. The convergent guns, on the other hand, were mounted outside the magnetic field. By means of a movable piston and bellows, the position of the convergent-gun assembly with respect to the shielding end plate could be conveniently adjusted. Exact constructional details are available in the references (1, 2) and will not be dealt with here.

Every part of the tube assembly had to be vacuum tight. Teflon or neoprene O-rings were employed between the different joints. A 4-inch, modified D. P. I., metal diffusion pump in conjunction with a glass booster pump and a mechanical forepump evacuated the entire system. An inverted liquid-nitrogen trap was used to condense any vapors present in the system. Two ionization gauges determined the pressure inside the vacuum tube. One gauge opened right into the gun chamber; the other was located near the cold trap. During the activation process, the pressure readings of the two gauges differed by orders of magnitude. After the cathode was well activated, however, both gauges indicated the same pressure. The best obtainable vacuum, as measured by a Bayard-Alpert ionization gauge (3), was 4×10^{-8} mm Hg. (Inside the drift tube proper, the pressure was probably higher by a factor of 7.) This pressure was obtained without baking out the system. Brass parts and the lubriseal of the sliding joints prevented all but mild heating of the tube assembly.

At the end of the drift tube, the electron beam entered a hollow collector. The collector was mounted outside the magnetic-field region. As a consequence, the beam spread to the inner walls of the collector. The chances of secondary electrons getting back into the drift tube were thus greatly reduced. The application of a small positive bias to the collector further reduced the secondary emission effect to a presumably negligible amount.

Approximate beam-diameter measurements could be made with a movable shutter. Holes of various sizes were drilled in the shutter. Rotating the shutter in the path of the beam permitted varying percentages of the collector current to be intercepted. The amount of the interception varied as a function of the intercepting hole diameter. From the magnitude of the interception and the intercepting hole diameter, the approximate beam diameter could be extrapolated.

A re-entrant cavity (1, 2), resonant at approximately 2734 Mc/sec, measured the noise current along the beam. The current modulation picked up by the cavity coupled to a rigid coaxial line. This coaxial output line passed into the surrounding atmosphere through a vacuum-tight sliding seal. With this arrangement, the cavity position could be easily varied from the outside, without adversely affecting the vacuum inside the tube. To facilitate the continuous recording of the results, a motor drive was devised which moved the cavity smoothly at any predetermined rate. The automatic cavity-moving mechanism is shown in Fig. 3.

2.3 GENERATION OF POSITIVE IONS

An electron beam in a long drift tube produces positive ions because of collisions of some electrons with remaining gas molecules. At normal operating pressures, there are enough ions generated to neutralize, at least partially, the otherwise negative space charge of the beam.

Spangenberg, Field, and Helm (4) showed that even though one might expect the beam in a drift tube to become fully neutralized at pressures as low as 10^{-7} mm Hg, measurements indicated a beam spread resulting from lack of full neutralization at pressures as high as 10^{-6} mm Hg. The lack of neutralization indicated that some unexpected loss of ions occurred. They ruled out recombination, wall charges, and increased gas temperature as potential causes for ion loss. Instead, they formulated a new theory based upon the idea of an ion sink along the beam. According to the ion-sink theory, a small external field penetrated a short distance into the otherwise field-free drift space and continuously removed ions from the beam in that region. The removal of ions in one section of the beam caused a potential depression at the center of that region and therefore attracted the positive ions from the nearby section. In this fashion, a mechanism was provided by means of which ions started to flow towards the sink. Ions were thus effectively removed from much greater distances than the original field penetration would have indicated. Since some stray fields could have penetrated into the drift tube from the nearby accelerating-gun region through the apertures, ions could be removed in the direction of the gun. The ion-sink theory is further justified by experimental results.

In the experiments reported here, the effect of the ion sink could be canceled and full neutralization of the beam obtained with the aid of a potential barrier. This potential barrier consisted of a ring-shaped electrode mounted a little beyond the aperture of the magnet shield. The ring was kept at a positive potential with respect to the drift region. It could, therefore, repel the approaching positive ions.

It takes a certain time to build up an ion core. Applying a pulse to the beam, the time to neutralize the beam fully is given (4) as $T = 4.56 \times 10^{-14}$ (V volts/P mm Hg). (The empirical ionization coefficient given in ref. 4 was in error (21) by a factor of 12.6 for 1500 volts. The equation given above was, therefore, corrected for that amount.)

Figure 4 shows the buildup time and the percentage neutralization as a function of pressure. The curves of Fig. 4 were computed with the assumption of no ion loss. A beam voltage of 1500 volts and a pulse duration of 0.7 μsec were used in the calculations. Neglecting ionization from sources other than collisions (cathode emission, soft X-rays, and so on), it became evident that negligible neutralization of the beam occurred in the neighborhood of 10^{-7} mm Hg for voltage pulses shorter than 1 μsec. Of course, the repetition rate had to be small enough so that the relatively few ions generated during the pulse would drift out of the beam between successive pulses.

With an increased pulse length, the beam could be measured with any degree of neutralization by adjusting the time delay between the leading edge of the pulse and the time of observation. Again, sufficient time had to be allowed for the complete removal of ions between successive pulses.

2.4 MODULATOR AND MEASURING EQUIPMENT

Since it was desired, among other things, to determine the effect of ion neutralization on the noise in electron beams, measurements had to be performed under both steady- and pulsed-beam conditions. Test setups had to be devised according to the modulation of the beam. At the outset of the experiments, the noise measurements were performed on steady-flow beams. The cavity output was fed through a variable waveguide attenuator into a waveguide coupler and a crystal mixer. A klystron local oscillator signal entered the same waveguide coupler. The two signals mixed and produced a 30-Mc/sec beat frequency. An i-f strip amplified the detected 30-Mc/sec component. After a second detection, the output could be monitored on a microammeter and an oscilloscope. The sensitivity of the detection method just described was relatively poor. Consequently, no accurate measurements could be made in the vicinity of the deeper noise minima along the beam. To increase the sensitivity, synchronous detection was used. Accordingly, the measuring apparatus was modified in a manner similar to that devised by Dicke (5) for the measurement of thermal radiation at microwave frequencies. Figure 5 shows the modified test setup. A thin lucite disk, approximately 25 inches in diameter, reached into a slotted section of waveguide. The disk was eccentrically coated with lossy paint. The distribution of paint was such that the rotating disk square-wave modulated the rf noise output of the cavity. Since the disk was driven by an 1800-rpm synchronous motor, the output contained a strong 30-cps component. This component was reamplified by a narrow-band, 30-cps lock-in amplifier and then allowed to beat against a 30-cps reference sine wave. The reference signal came from a 30-cps generator which was mechanically coupled to the modulator disk. The phase of the generator could be adjusted for maximum sensitivity. The output appeared on a milliammeter. The receiver sensitivity was increased by about 15 db in this fashion. Reliable measurements in the region of the noise minima were thus possible. However, data were obtained – and some of them will be included in this

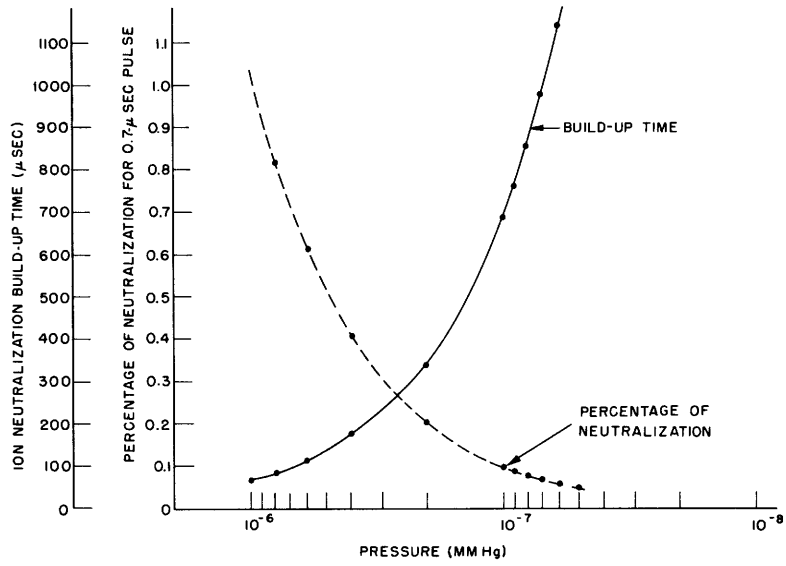

Fig. 4. Neutralization time and percentage neutralization caused by collisions at 1500 volts.

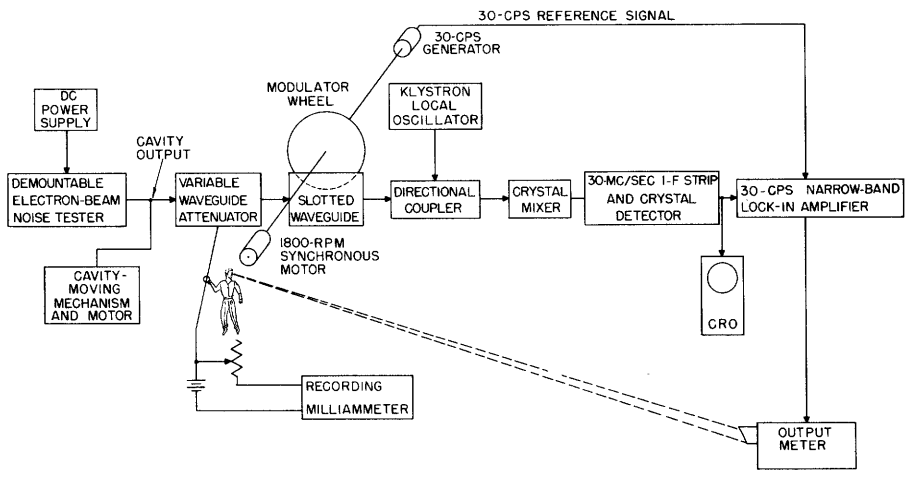

Fig. 5. Block diagram of apparatus used in measuring the noise in steady-flow electron beams.

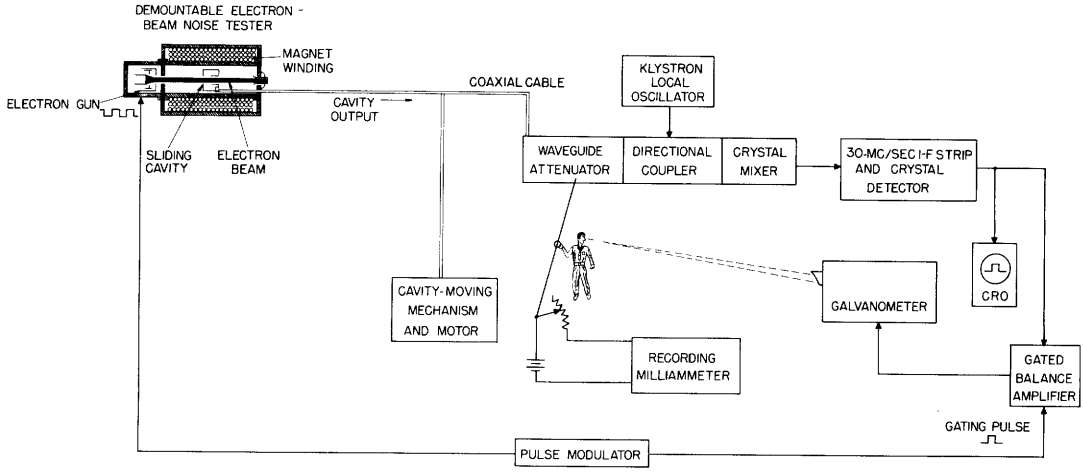

Fig. 6. Block diagram of apparatus used in measuring the noise in pulsed electron beams.

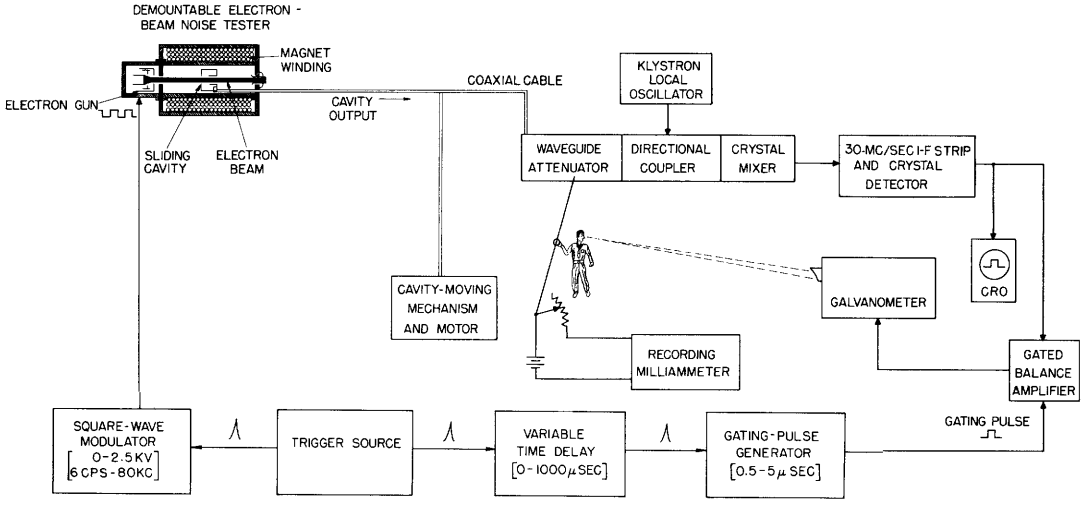

Fig. 7. Block diagram of apparatus used in measuring the noise with variable neutralization of electron beams.

paper – even before the synchronous modulation detector was designed and put into operation.

For the investigation of Brillouin-flow (6), it became necessary to make measurements on unneutralized electron beams. Previous calculations concerning positive-ion generation showed that the neutralization amounted to less than 1 per cent when the beam was pulsed for a duration of 1 μsec or less. A hard-tube modulator was used to pulse the beam. The pulse duration was 0.7 μsec with a repetition rate of 4000 cps. Two considerations determined the lower and upper limits of the repetition rate. First, the time interval between successive pulses had to be sufficiently long to allow the removal of the ions already present in the drift tube. On the other hand, the repetition rate had to be high enough to bring the average noise power above the noise level of the receiver. If it is assumed that the pulsed noise power induced in the probing cavity was of the same order of magnitude as under steady-beam conditions, the average noise power would be approximately 24 db less for a 4000-cps repetition rate. Since this was less than the noise level of the receiver, it was necessary to gate the output circuit as indicated in Fig. 6. Considerable time and effort were spent in shielding and suitably grounding every piece of equipment in order to keep the modulator video pulse from swamping the receiver.

The experiments indicated a marked difference in the results, dependent on whether the noise measurements were performed on pulsed (almost unneutralized) or steady-flow (entirely or almost neutralized) electron beams. To close the gap between the two operating conditions, the following experiment was devised. A long (several hundred to several thousand microseconds) voltage pulse produced a beam that was unneutralized at the beginning, but reached its final degree of neutralization toward the end of the pulse. By applying a gate of short duration to the noise output, with various time delays after the leading edge of the pulse, it was possible to make sets of intermediate measurements between unneutralized and neutralized conditions. Figure 7 shows a block diagram of the apparatus used in performing this type of experiment. Since a pulse modulator generating pulses several hundred microseconds long and 2500 volts in amplitude at a 50 per cent duty cycle was not readily available, a 2.5-kv dc power supply was modified to do the job. With the aid of a switching circuit and a condenser bank, the modulation requirements were satisfactorily realized. The output reproduced the pulse duration and the repetition rate of an input generator. Since an input pulse of 40 volts in amplitude was sufficient, most available square-wave or other pulse generators could be used for the input. The output pulse height was independent of the input and could be continuously adjusted from 0 volts to 2500 volts. The output pulse had a rise time of approximately 1.5 μsec and was flat, without any drooping, up to several thousand microseconds duration. The input pulse shape had no effect on the output.

A Radiation Laboratory (M.I.T.) TGP-6SE pulse generator provided a gating pulse which was adjustable from 0.5 μsec to 5 μsec. The gating pulse could be delayed from 0 μsec to 1000 μsec with the aid of a DuMont 256-D A/R oscilloscope. A gated balance

amplifier was specially designed (7) and built to eliminate receiver noise between pulses.

2.5 TECHNIQUE OF MEASUREMENTS

After activation of the cathode, the beam focusing was adjusted to reduce the interception current. The minimization of interception current was necessary in order to eliminate partition noise (8, 9) as much as possible. For reasonable values of the collimating magnetic field, over 99.9 per cent of the cathode current reached the collector. With less than 0.1 per cent interception current, the partition noise was assumed to be negligible, and the total of the measured noise could be attributed to conditions in the beam proper.

A simple method was devised to facilitate the fast, continuous recording of the noise current along the beam, even though the final output was often not more than a few microvolts. As the block diagrams show, the cavity output was always fed first through a variable waveguide attenuator. The amplified and detected noise output appeared finally on a dc ammeter or galvanometer. As the cavity position was changed by the automatic mechanism shown in Fig. 3, the output reading was kept constant by manual adjustment of the waveguide attenuator at the input. The angular displacement of the attenuator control knob was mechanically coupled to the shaft of a helipot. This potentiometer was in series connection with an Esterline-Angus recording milliammeter and a battery. The current through the recorder varied in a hyperbolic manner with the potentiometer setting. This variation bucked the nonlinearity of the attenuation as a function of attenuator displacement. Consequently, the recorded output appeared almost linear on a decibel scale.

The noise-output curves were calibrated relative to pure shot noise in the beam. The method of calibration was originally used by Cutler and Quate (10). This method consisted of lowering the cathode temperature until the collector current became temperature limited. Under temperature-limited conditions, the noise became directly proportional to the current. Thus, plotting the output in decibels against the current on a semilogarithmic scale yielded a straight line for the temperature-limited region. By extending the straight line into the space-charge-limited domain, the noise output could be easily calibrated relative to pure shot noise. Since space-charge waves (11,12) were supported by the beam even under conditions of temperature-limited emission, the cavity had to be kept close to the anode during the calibration procedure.

III. MEASUREMENTS ON CONVERGENT-FLOW BEAMS

3.1 INTRODUCTION

Convergent-flow electron guns are often used to produce high-current-density electron beams. The radial forces caused by the space charge can be balanced by an axial magnetic field. Under ideal Brillouin-flow (6, 13) conditions, the beam originates outside the magnetic field and converges to a certain minimum diameter. In the plane of

the minimum beam diameter the electrons do not have any radial velocity components. If an abruptly rising magnetic field is applied at the minimum beam diameter, then for a certain specified field strength the beam should maintain the entrance diameter throughout the drift region. The value of the critical field is the so-called Brillouin field. It is assumed that the beam is unneutralized so that a balance can exist between the outward-acting space-charge forces and the inward forces produced by the magnetic field. Violation of the requirements for Brillouin-flow would result in a beam contour that is scalloped, instead of cylindrical. Moster and Molnar (14) investigated the possibility of obtaining Brillouin-flow with nonabruptly rising magnetic fields. They found that Brillouin-flow is theoretically possible, provided the magnetic shield is properly located. The field strength has to be somewhat stronger than the Brillouin field. Consequently, the final beam diameter is sometimes reduced by as much as 30 per cent. According to Moster and Molnar, larger magnetic fields can produce little further squeezing of the beam if the entrance conditions are correct.

This section gives a detailed description of the beam-shape measurements on convergent-flow electron beams. The latter part of the section contains the results of noise measurements. These noise measurements were also performed on convergent-flow beams. The effect of substituting Philips cathodes for the usual oxide-coated ones is also discussed.

3.2 BEAM CONTOUR MEASUREMENTS

The initial measurements were performed on beams produced by oxide-coated cathodes in a Pierce gun with the following parameters:

Perveance	0.083×10^{-6}	amp/volt$^{3/2}$
Cathode diameter	0.130	inch
$\overline{r_a}$	0.236	inch
$\overline{r_c}$	0.530	inch
r_{min} (theoretical)	0.010	inch
θ (half angle of convergence)	7.2°	

The minimum beam diameter and its distance from the anode were computed from the curves given by Pierce (6). Moster's and Molnar's (14) data were used to determine the correct anode spacing from the magnetic shield. The calculation accounted for the gradual rise of the magnetic field and the lens effect of the shield aperture. However, it was found experimentally that the anode had to be moved considerably closer to the shield for optimum focusing than predicted by calculations. The beam contour was measured with the aid of the shutter attached to the movable cavity. By moving any one

of the shutter holes into the path of the beam, electrons in the periphery of the beam were intercepted. The core of the beam passed through unhindered to the collector. The beam diameter could be easily computed from the percentage beam transmission through any known hole, if uniform current-density distribution across the beam were assumed. As the shutter moved along the beam, the variations of the interception or collector current indicated the changes in the beam contour. Though the assumption of uniform current-density distribution over any cross section of the beam was debatable, the experiment just described did give the approximate beam diameter and a very good measure of the variation of that diameter as a function of distance along the beam.

To minimize ionization effects, the beam was pulsed for approximately 0.7 μsec with a repetition rate of 4000 cps. Previous calculations showed that less than 1 per cent of the beam would become neutralized under those conditions. The beam diameter was measured carefully for various magnetic fields. The position of the gun with respect to the shield was also optimized to obtain a smooth, cylindrical beam. In spite of all efforts, however, the beam contour remained somewhat scalloped. At best, the observed beam diameter variations were of the order of 10 per cent, if uniform current-density distribution was assumed across the beam. The measured wavelength was shorter than the theoretical value for perturbed Brillouin-flow. The length of the scallops was approximately 1.1 times that of the cyclotron wavelength instead of the predicted $(2)^{1/2} \lambda_c$. The average beam diameter was approximately 0.043 inch; that is, a little over twice the value calculated from Pierce's curve (6). However, that particular graph did not take into account the effect of thermal velocities as a limiting factor in the computation of minimum beam diameters. In the same reference, Pierce also showed how to determine the voltage at which the thermal-velocity limitation equaled that of the space charge. For the gun parameters given before, this "borderline" voltage was approximately 700 volts. Above 700 volts, the space-charge limitation dominated that of the thermal velocities; below 700 volts, the opposite was true.

The contour measurements were repeated for steady-flow convergent beams. As before, the beam was scalloped for all values of magnetic field and gun position. The perturbation wavelength was 1.1 λ_c, the same as that recorded under pulsed-beam conditions. The beam diameter, however, was smaller this time. Since a steady-flow beam is at least partially neutralized, the reduction of beam diameter did not come as a surprise. In a neutralized beam, the outward-acting space-charge forces are effectively counteracted by positive ions, and a thinner beam could be realized.

For a beam diameter of 0.043 inch, a pulse amplitude of 1500 volts and a peak current of 4.8 ma, a Brillouin field of approximately 170 gauss was calculated. In practice, however, the collimating field had to be almost twice as large. The increased field strength was necessary to reduce the interception current below 0.1 per cent. Figure 8 shows typical interception-current curves for various values of the magnetic-field strength. Sometimes minute negative interception current resulted. The negative interception current could originate in at least two ways. First, with every positive

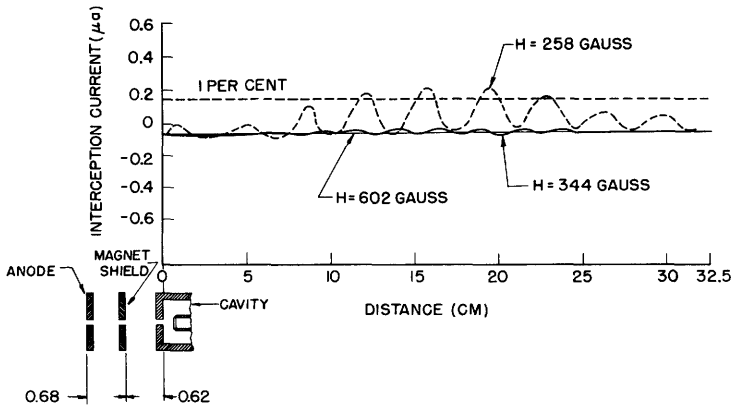

Fig. 8. Interception current versus cavity position for convergent-flow pulsed electron beam. V_o = 1500 volts; $I_{collector}$ = 16.6 μa; pressure $\approx 7 \times 10^{-7}$ mm Hg.

ion generated by collision a secondary electron was released. If the number of positive ions contributing to the interception current exceeded the sum of the primary and secondary electrons intercepted by electrodes other than the collector, the resulting interception current would then be negative. The other explanation is based upon the assumption that primary electrons were intercepted by the copper parts of the cavity. Since, at the operating voltages used, the secondary emission coefficient of copper was greater than one, negative interception-current readings were possible. To minimize partition noise, the focusing was adjusted for least interception. Thereafter, the noise current in the beam was measured for various values of beam voltage, magnetic field, neutralization, and cathode temperature.

3.3 NOISE MEASUREMENTS ON STEADY-FLOW BEAMS

A number of noise-current curves were recorded as functions of distance along the drift tube. Figures 9, 10, and 11 show a few sets of these curves for accelerating voltages of 700, 1000, and 1500 volts, respectively. The magnetic field was the varying parameter on all three figures.

The space-charge wavelength became longer for increasing voltages. This observation could be expected from theoretical considerations. The calculated space-charge wavelengths were 14.8 cm, 16.8 cm, and 19.7 cm for V_o = 700, 1000, and 1500 volts, respectively. These values are in very good agreement with the measurements 13.8 cm, 15.6 cm, and 19.6 cm shown in Figs. 9, 10, and 11. To make the comparison, the curves with H = 430 gauss should be used because the beam-diameter measurements were performed at that magnetic field. The magnitude of the standing-wave ratio varied from 10 db to 13 db at lower magnetic fields to 5 db to 7 db at higher field strengths. The reduction in the standing-wave ratio at the stronger fields was the result of raising the noise-wave minima and simultaneously lowering the maxima.

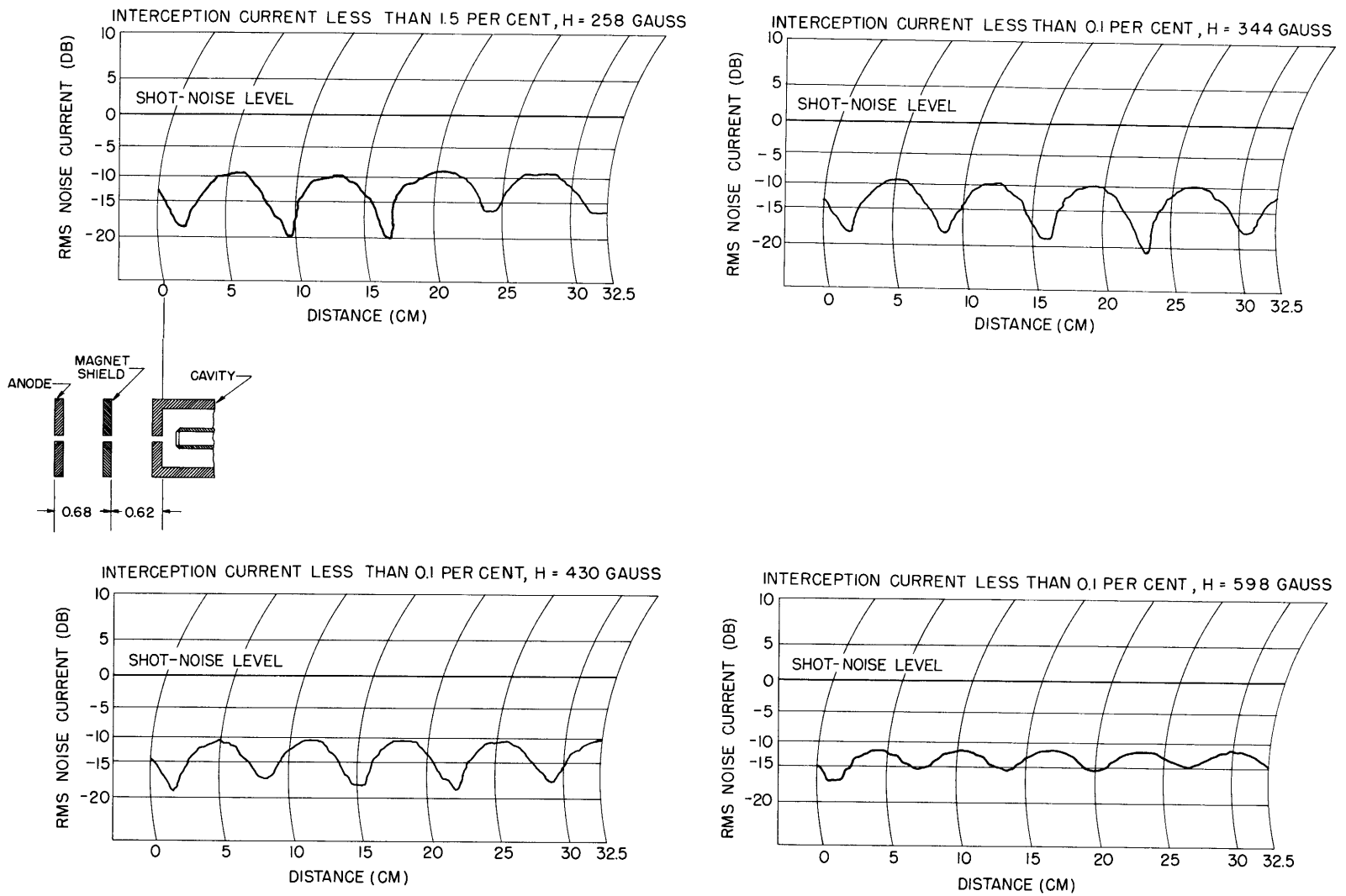

Fig. 9. RMS noise current versus cavity position for convergent, steady-flow electron beam. $I_{collector} = 1.7$ ma; $V_o = 700$ volts; pressure $\approx 4.5 \times 10^{-7}$ mm Hg; beam diameter ≈ 0.035 inch.

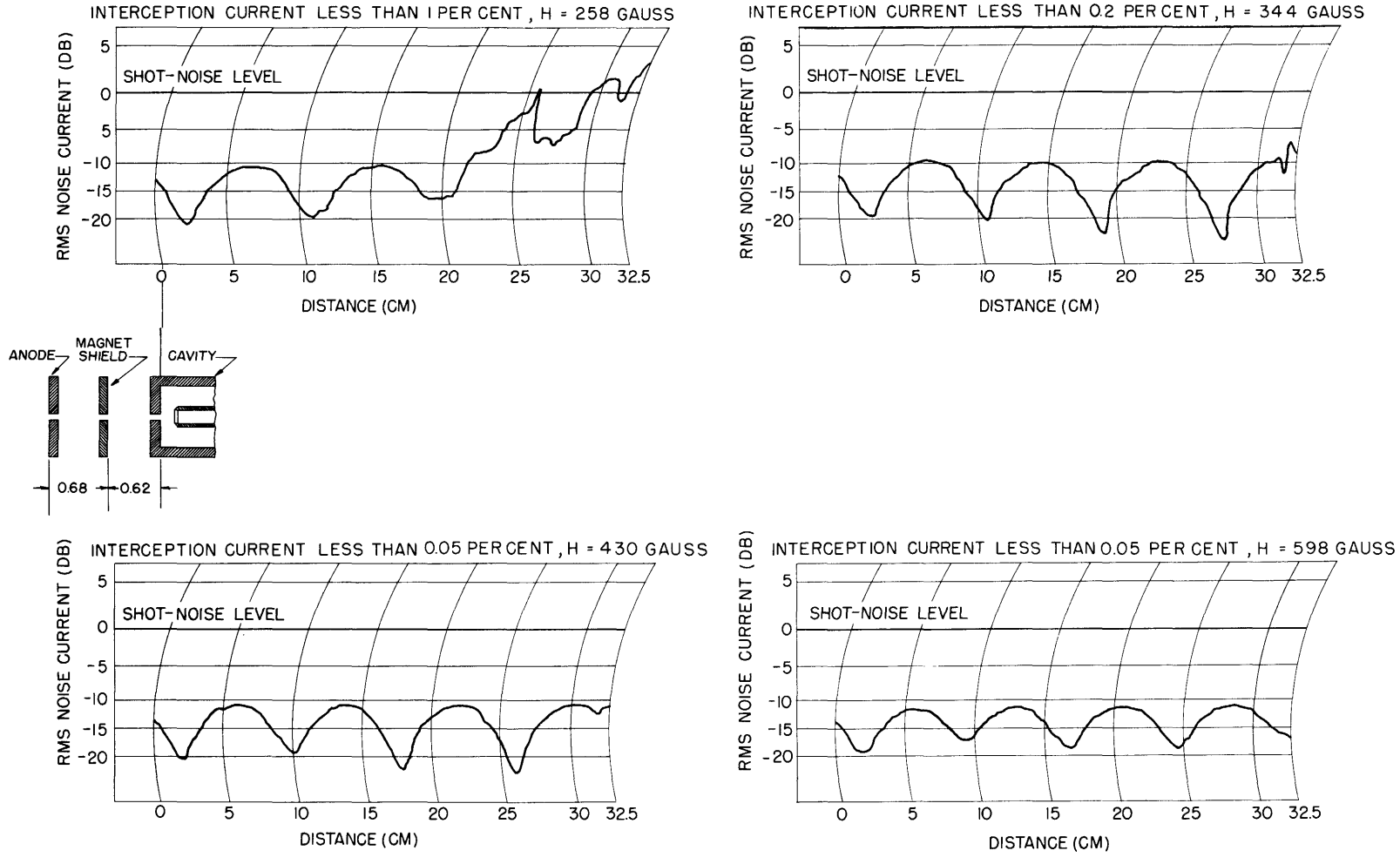

Fig. 10. RMS noise current versus cavity position for convergent, steady-flow electron beam. $I_{collector} = 2.8$ ma; $V_o = 1000$ volts; pressure $\approx 5 \times 10^{-7}$ mm Hg; beam diameter ≈ 0.035 inch.

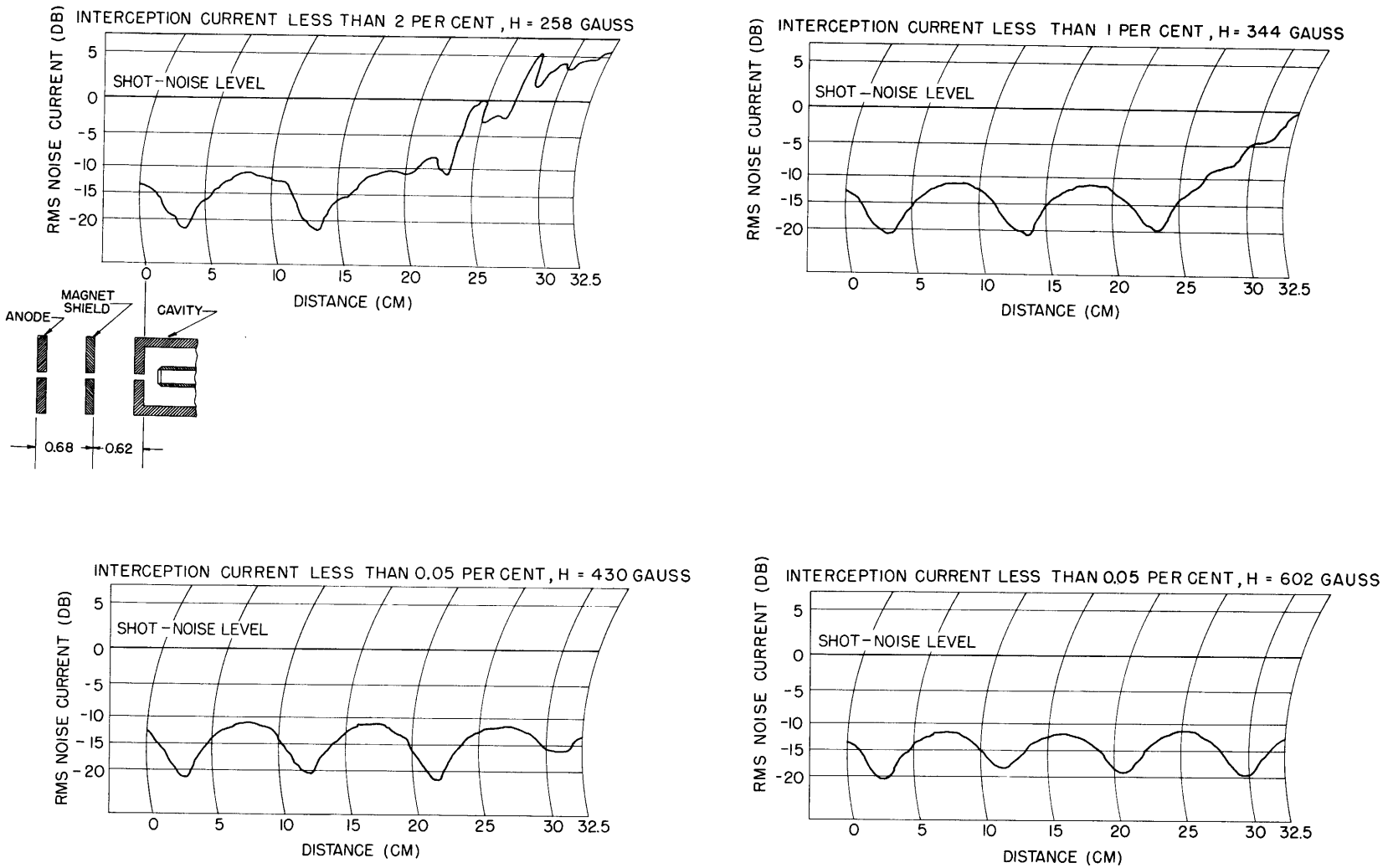

Fig. 11. RMS noise current versus cavity position for convergent, steady-flow electron beam. $I_{collector} = 4.8$ ma; $V_o = 1500$ volts; pressure $\approx 8 \times 10^{-7}$ mm Hg; beam diameter ≈ 0.035 inch.

Growing noise waves were also observed under certain conditions. Assuming that the noise-current curves consisted of a periodic standing wave and a superimposed growing wave, we observed a spatial delay of the growing part as the magnetic field increased. For very large magnetic fields, the growing part of the noise wave disappeared altogether from the drift space under observation. It might well be that in a longer drift tube the growing part would still be evident.

3.4 NOISE MEASUREMENTS ON UNNEUTRALIZED BEAMS

The measurements were performed under pulsed operation in order to avoid neutralization of the beam. A pulse duration of 0.7 μsec was used with a 4000-cps repetition rate. The generated pulse had a very short rise time and no observable overshoot. While the rise time amounted to only a fraction of a microsecond, the fall time was appreciable. Figure 12 illustrates a set of noise-current curves obtained by using 1500-volt pulse amplitudes. The magnetic field was again the varying parameter. The pulsed noise-current curves had the same general characteristics as the ones for steady-flow beams. The growing part, however, was appreciably larger for the unneutralized beam. It therefore seemed improbable that the ions present in the beam caused the growing noise wave. This belief was further strengthened by other experiments; the additional evidence will be discussed later. The minima, with the exception of the first one, were rather ill-defined, compared to Fig. 11. Since the space-charge wavelength changed for different beam voltages, the relatively long fall time of the voltage pulse could have smeared the minima. All curves, including the fine structure, were well reproducible. A considerable amount of instability was present, however, in the growing part of the noise wave for levels greater than approximately 10 db above shot noise.

The noise measurements discussed so far were all performed on space-charge-limited electron beams. The measurements were repeated after lowering the cathode temperature to produce temperature-limited beams. Figure 13 shows the noise measurements for the temperature-limited case. Again, the magnetic field was the varying parameter and 1500 volts the pulse amplitude.

Figure 13 shows the existence of growing noise waves even in temperature-limited electron beams. A rise up to approximately 15 db above the shot-noise level could be observed. A spatial delay of the growing portion was again noticeable for increasing magnetic fields.

3.5 NOISE MEASUREMENTS ON BEAMS WITH VARIABLE NEUTRALIZATION

The results of this section indicate differences in the magnitude of the growing wave and the number and deepness of the minima before the growing part set in. Under pulsed conditions there was a much stronger tendency toward growing noise wave in the second half of the drift tube than with steady-flow operation. To close the gap between these two operating conditions, the following experiment was devised. Pulsing the beam with a very long voltage pulse produced a beam that was unneutralized at the beginning, but

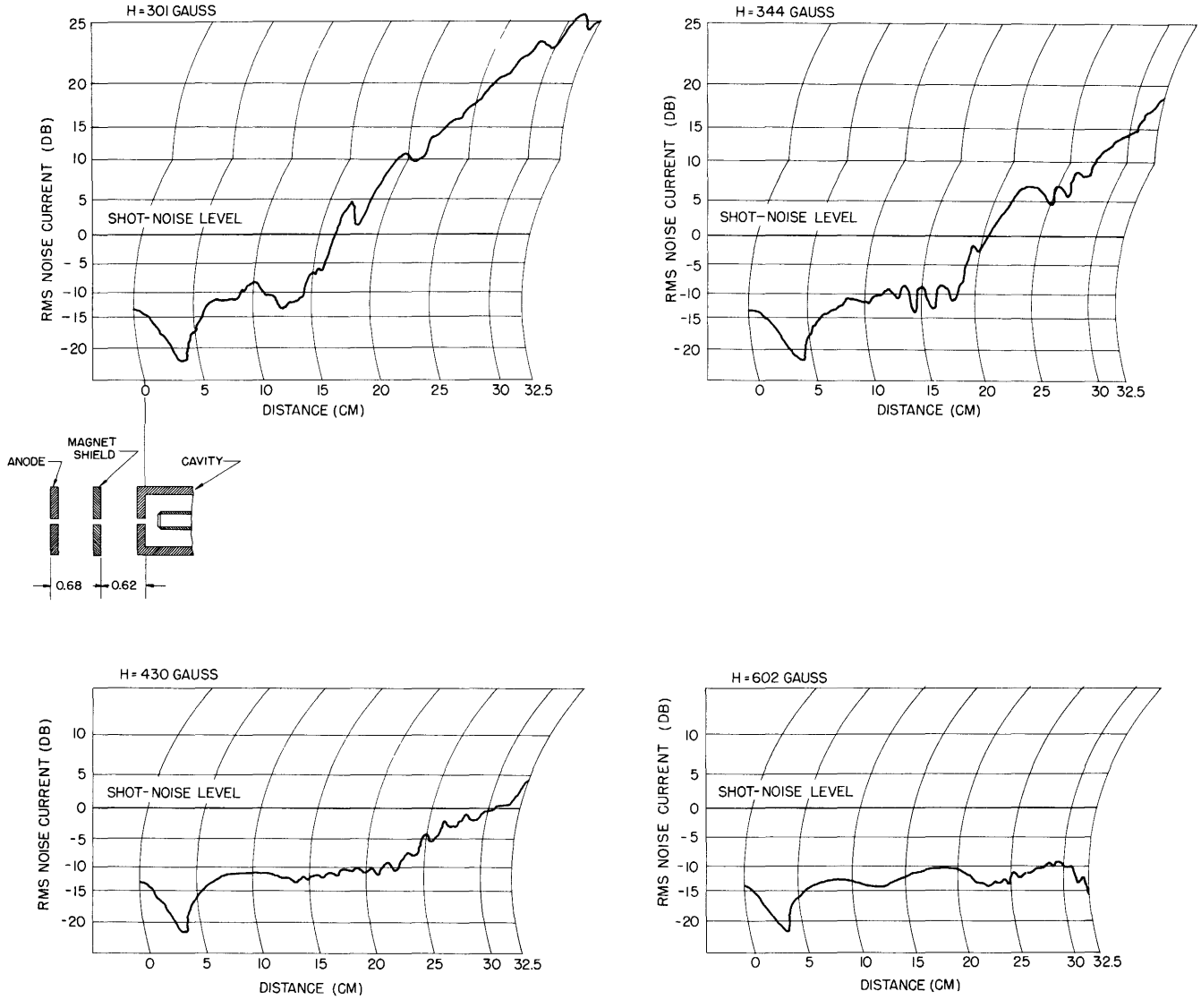

Fig. 12. RMS noise current versus cavity position for convergent-flow pulsed electron beam. $I_{collector} = 16.6\ \mu a$; $V_o = 1500$ volts; pressure $\approx 7 \times 10^{-7}$ mm Hg; beam diameter ≈ 0.035 inch.

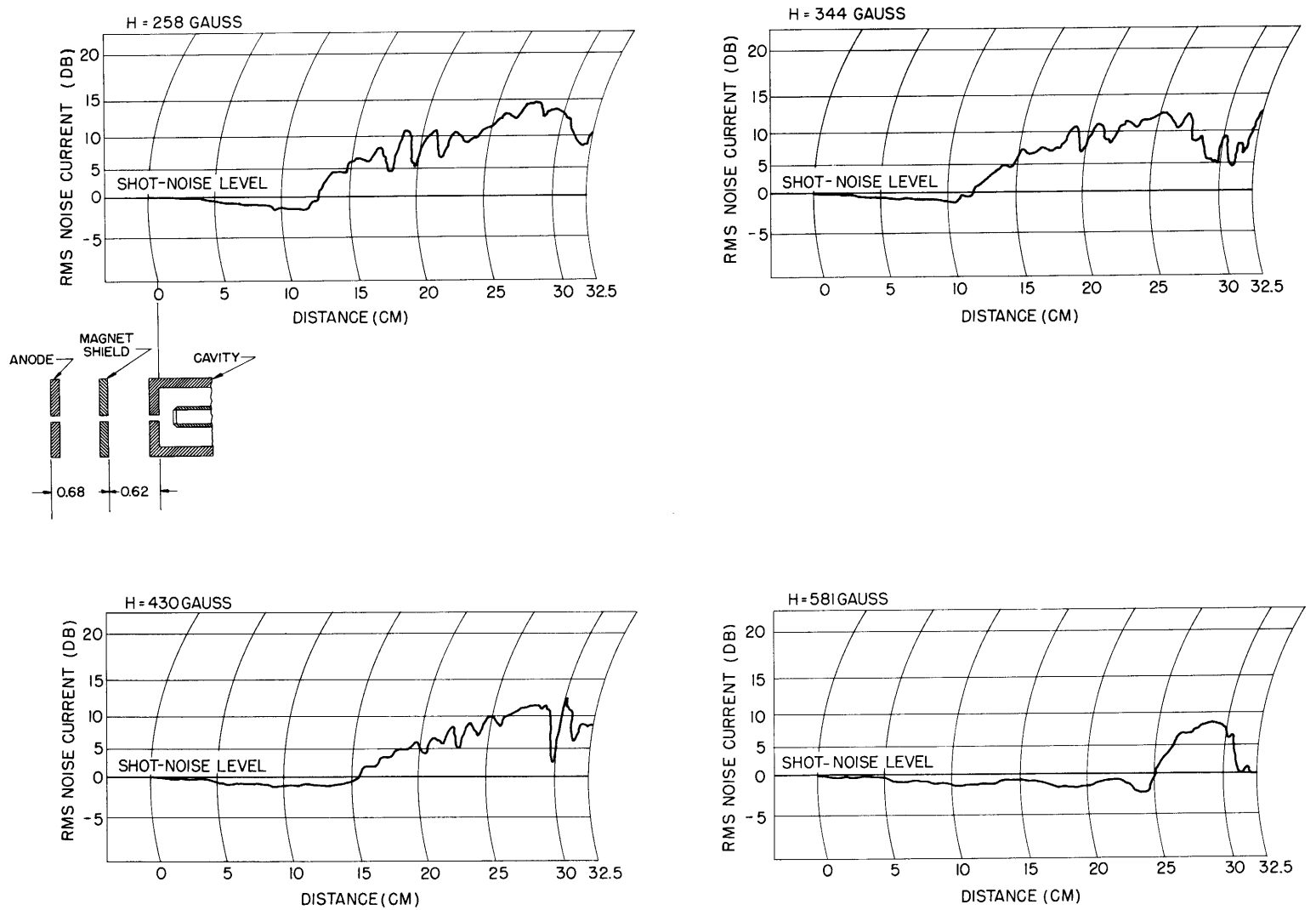

Fig. 13. RMS noise current versus cavity position for temperature-limited pulsed electron beam. $I_{collector} = 1.1$ μa; $V_o = 1500$ volts; pressure $\approx 7 \times 10^{-7}$ mm Hg.

reached its final degree of neutralization toward the end of the pulse. By applying a gate of relatively short duration to the noise output with various time delays after the leading edge of the pulse, it was possible to make sets of intermediate measurements between unneutralized and neutralized conditions. The apparatus used to perform this experiment was illustrated in Fig. 7. The pulse modulator maintained a 50 per cent duty cycle with a variable repetition rate and voltage. The pulses were very flat and had a rise time of approximately 1.5 μsec. The Pierce gun was the same as that used in previous experiments.

The modulator pulse length was first adjusted to 500 μsec. An approximately 3.5-μsec gating pulse was applied after time delays of 4, 14, 104, and 304 μsec. In later experiments, the modulator pulse length was increased to 2500 μsec and the gating pulse shortened to approximately 1.5 μsec. The time delays in the latter case were 0, 4, 104, and 1004 μsec. The delay was measured from the time when the modulator pulse reached its final amplitude; that is, approximately 1.5 μsec to 2 μsec after the start of the pulse. The resulting noise-current curves are shown in Figs. 14 and 15, respectively. In both figures, the magnetic field and the gating-pulse time delays were the varying parameters. The magnetic field increased from left to right, while the downward direction represented longer time delays. The interception current was measured independently of the noise. It was found that the maximum value of the interception did not exceed 0.1, 0.1, 0.2, and 1.5 per cent of the collector current for magnetic fields of 602, 430, 344, and 258 gauss, respectively.

Figure 15 illustrates very well that the growing part of the noise wave decreases considerably for increasing neutralization. Figure 14 represents the same general trend. However, the transition is not as clear cut, probably because the time delays were too closely spaced and did not cover a sufficiently wide range. Also, 500 μsec was probably insufficient for the removal of all the ions generated by a current pulse. Since there was no external field, the ions had to drift to the surrounding walls because of their own space-charge forces and initial velocities.

The magnitudes of the growing waves in Fig. 15 bridged over half of the gap which existed between those of Fig. 11 (steady-flow measurements) and Fig. 12 (0.7-μsec pulse measurements). The noise-current curves as measured after at least a 100-μsec time delay were in excellent agreement with those of Fig. 11. A rather interesting attempt was made to extrapolate from the curves of Fig. 15 to those of Fig. 12. When doing so, we remembered that for the curves of Fig. 15 the rise time of the modulator pulse was approximately 1.5 μsec to 2 μsec, the gating pulsewidth approximately 1.5 μsec, and that the delay was measured from the time when the modulator pulse attained its final amplitude. Thus, the curves with time delays of 0, 4, 104 μsec, etc., were effectively measurements at approximately 0 + 2.5 μsec, 4 + 2.5 μsec, 104 + 2.5 μsec, etc., after the beam was started. Similarly, in place of the finite pulsewidth that was used with the curves of Fig. 12, we could assume that the measurements were taken 0.3 μsec after the pulse was initiated. With these facts in mind, the

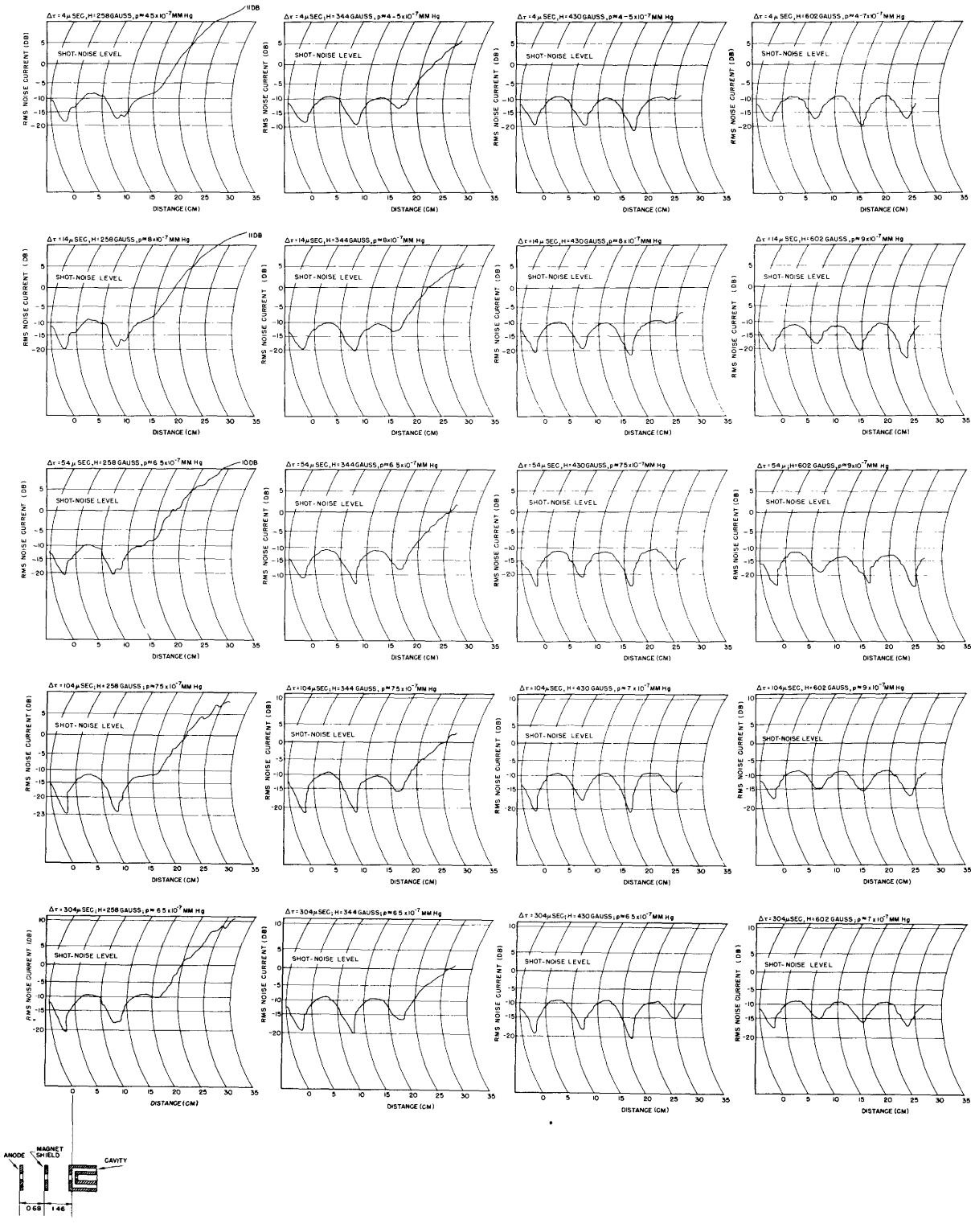

Fig. 14. RMS noise-current characteristics of a convergent-flow beam with variable degree of neutralization. V_o = 1500 volts; I_o = 4.7 ma; pulse duration, 500 μsec.

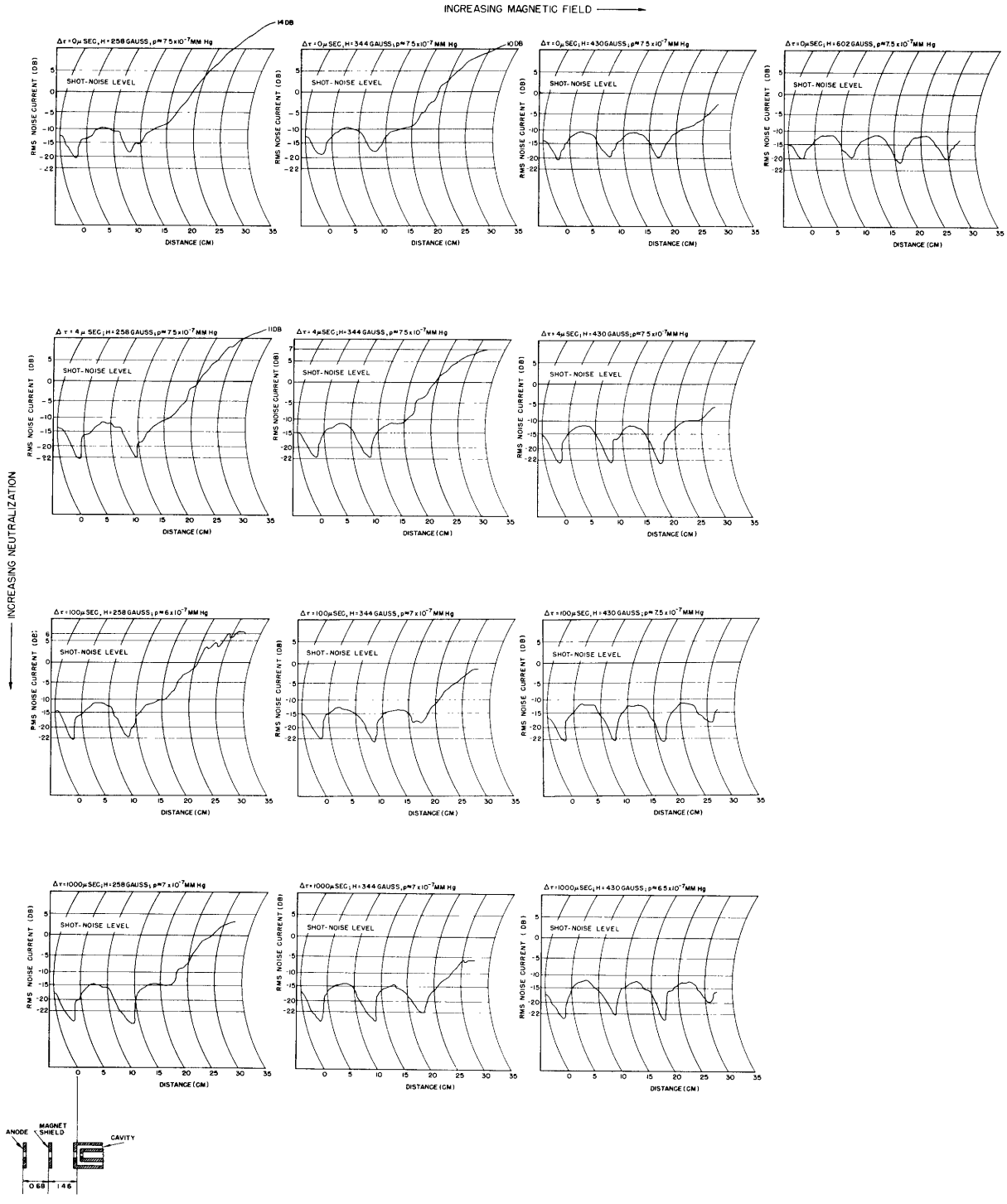

Fig. 15. RMS noise-current characteristics of a convergent-flow beam with variable degree of neutralization. V_o = 1500 volts; I_o = 4.7 ma; pulse duration, 2500 μsec.

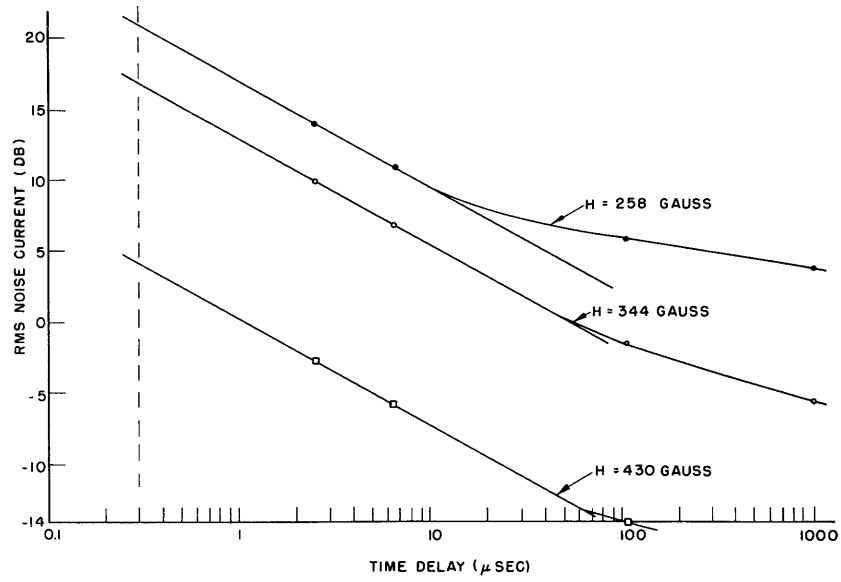

Fig. 16. Extrapolation of the growing noise waves at the end of the drift tube.

noise currents at the end of the drift space of Fig. 15 were plotted against time delay for H = 258, 344, and 430 gauss. The resulting curves were then extrapolated to 0.3 μsec as shown in Fig. 16. A straight line extrapolation through the points at 2.5 μsec and 6.5 μsec seemed reasonable even though somewhat arbitrary. The surprising thing, however, was that the resulting intercepts at 0.3 μsec were in very good agreement with the corresponding noise values of Fig. 12. Another startling observation was that the straight lines of extrapolation were parallel. There were indications that guns having the same perveance but using impregnated Philips cathodes gave qualitatively similar results and yielded extrapolation lines approximately parallel to those of Fig. 16; however, the data available for the Philips cathodes were insufficient for making a definite statement at this time. The temptation was rather great to write down an empirical relation which described the observations of Fig. 16. After transformation from log-log into linear scale, the noise current of the growing wave could be described from Fig. 16 as

$$\overline{i^2} = \frac{10^{B/10}}{t^{A/10}}$$

where $\overline{i^2}$ is the rms noise current in the growing wave, t is the time in microseconds, B is the intercept on Fig. 16, and A is the slope of extrapolation line in Fig. 16. In the equation given above, B varied inversely with pressure and magnetic field while the degree of neutralization increased directly with time. The value of A remained invariant for the conditions of Fig. 16. While avoiding premature conclusions, it could be

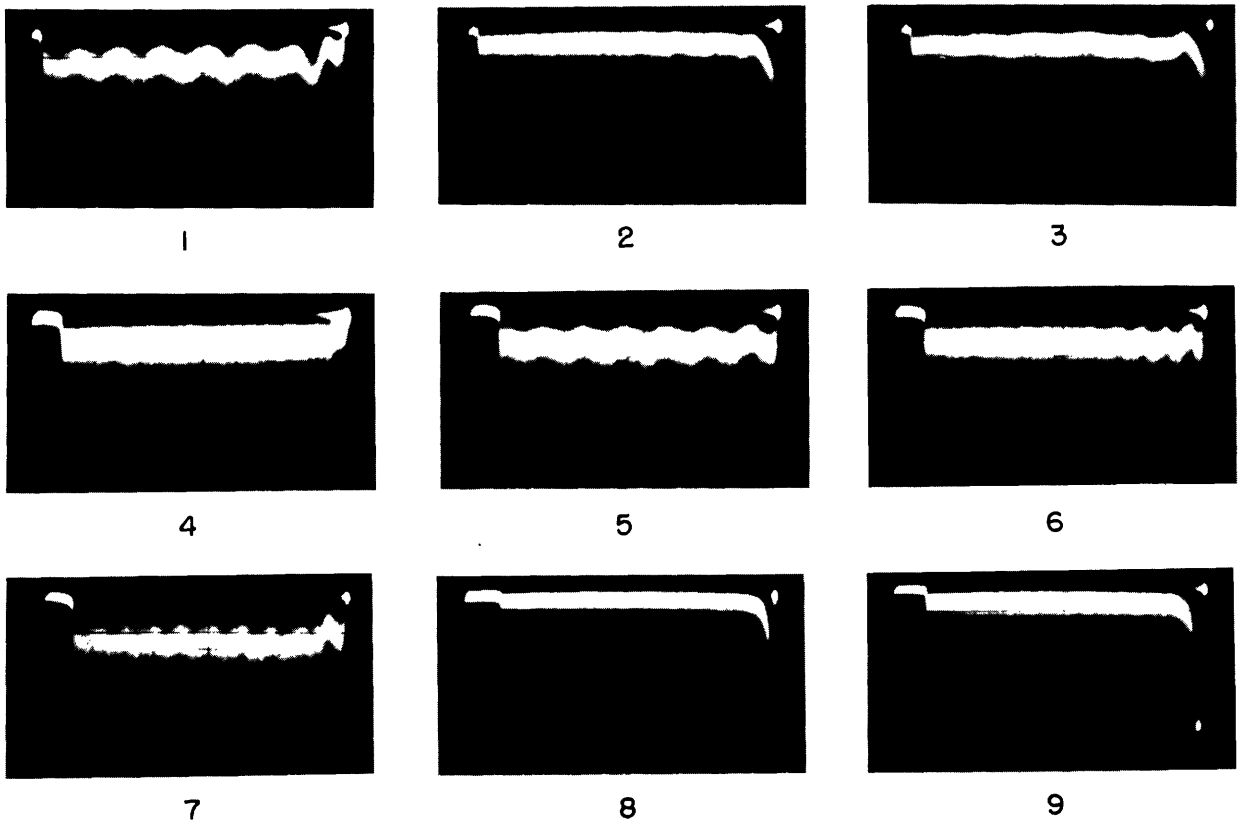

Fig. 17. Noise-current oscillograms of pulsed, convergent-flow electron beam. V_o = 1500 volts; I_o = 4.6 and 4.8 ma for heater voltages of 7.7 and 8.2 volts, respectively.

Picture	Magnetic Field (gauss)	Pressure (mm Hg)	Heater Voltage	Cavity Position (cm)
1	430	4.5×10^{-7}	7.7	29.1
2	344	4.5×10^{-7}	7.7	29.1
3	258	4.5×10^{-7}	7.7	29.1
4	602	3.5×10^{-7}	8.2	29.1
5	258	3.5×10^{-7}	8.2	29.1
6	258	$3.5 \times 10^{-7} \rightarrow 2 \times 10^{-6}$	8.2	29.1
7	258	4×10^{-7}	8.2	22.1
8	344	4×10^{-7}	8.2	22.1
9	344	4×10^{-7}	8.2	22.1

For all pictures, the sweep duration is 500 μsec. Zero time is on the right. The time increases from right to left. When taking picture 6, the pressure was increased about tenfold during the exposure time. Cavity position is measured from the anode.

definitely stated that by increasing the magnetic field or the percentage neutralization, the growing part of the noise decreased or even disappeared in all cases observed for convergent-flow electron beams.

A number of other interesting phenomena were observed in connection with the long-pulse experiments. Some of them are illustrated by the oscillograms of Fig. 17. The pictures were photographed under conditions corresponding to those of Fig. 14. Therefore, the time scale of the oscillograms was 500 μsec for full sweep. The distance scale of Fig. 14 also applied to all photographs. While no explanation is attempted at this time, the following observations are offered. Under certain critical conditions, oscillation-like ripples appeared on the scope. The ripples seemed continuous at first sight. Closer inspection revealed, however, possible intermittent, high-frequency oscillations with a relatively low repetition rate. The number of ripples usually corresponded to frequencies in the 5 kc/sec to 50 kc/sec range. The observability and the number of ripples were critically affected by pressure, magnetic field, beam voltage, and cathode temperature. For instance, a 5-10 per cent variation of the magnetic field could change the number of ripples by a factor of 2 to 3. Increasing the pressure or trapping the ions in the drift tube could wipe out the observed oscillations completely. The trapping of the ions was always a very efficient way to decrease the growing wave in convergent-flow beams with no detrimental effect on the noise standing wave.

3.6 MEASUREMENTS ON CONVERGENT GUNS WITH PHILIPS CATHODES

Most of the measurements described so far in this section were repeated with impregnated Philips cathodes. Independent measurements were made on two standard 3-mm cathode buttons. The gun dimensions were the same as those used in the previous convergent-flow experiments.

The observed results could be summarized as follows. The beam focusing was not as good as it was with the oxide-coated cathodes. In other words, larger collimating fields were necessary to keep the interception current down. For magnetic fields of 301, 430, and 602 gauss, the maximum interception current amounted to approximately 3, 1, and 0.5 per cent of the collector current. Only one-tenth of the values given above were obtained for the same magnetic fields when oxide-coated cathodes were used. The measured maximum beam diameter was larger for the Philips cathodes. Of course, their operating temperatures were approximately 300°C higher than those of the oxide-coated cathodes. In spite of these facts, the noise characteristics of the Philips cathodes were the same and in some respects considerably better than those of the oxide-coated ones. To be more specific, the space-charge wavelength, the noise-standing-wave ratios, the values of the standing-wave maxima and minima were in very good agreement for both types of cathodes. The surprising thing was, however, that the growing part of the noise wave was 4 db to 10 db less for Philips cathodes. The operating pressures during the Philips cathode experiments amounted to only about one-third of the pressure observed during corresponding experiments with oxide-coated cathodes.

This brought out even more clearly the fact that the tendency toward growing noise wave was considerably weaker with Philips cathodes than with oxide-coated ones.

For the growing part of the noise waves, oscillograms were made which displayed characteristics similar to the ones shown in Fig. 17. Trapping the ions, or increasing the pressure or the magnetic field, again helped to reduce the growing noise wave.

3.7 EFFECT OF MAGNETIC FIELD AT THE CATHODE

Measurements indicated that the main focusing field of several hundred gauss produced a leakage field of a few gauss at the cathode, outside the magnetic shield. Stray fields could also be introduced by nonbifilar heaters. To cancel or control the field strength in the cathode region, an auxiliary solenoid was placed around the gun outside the main focusing field. Earlier in this section we described strong growing noise waves in the latter part of the drift space. With a relatively weak (8 gauss to 15 gauss in the axial direction) auxiliary magnetic field in the gun region, the growing noise waves could be eliminated at will. While an auxiliary field of either polarity reduced the growing noise wave, smaller field strength was required if the axial components of the auxiliary and main focusing fields were similarly directed. The value of leakage field of the main solenoid was approximately 2 gauss to 4 gauss at the cathode. Typical growing-noise-reduction curves for a fixed cavity position as functions of the auxiliary field are shown in Fig. 18. The main focusing field is the parameter for the curves of Fig. 18. The convergent-flow gun used in these measurements had a bifilar heater. The parameters of this gun were given previously in section 3.2.

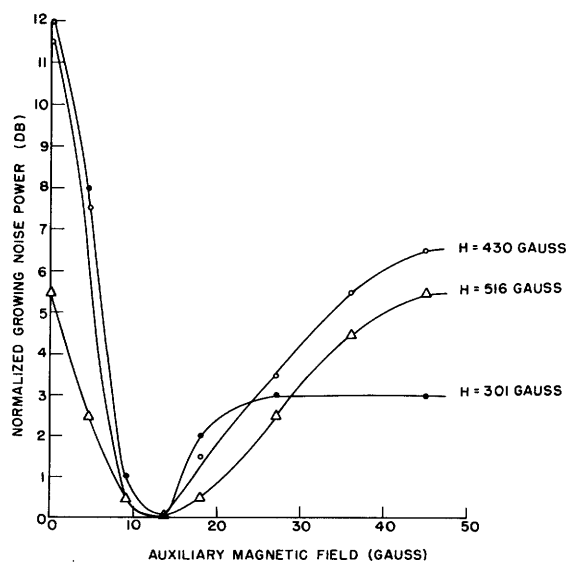

Fig. 18. Reduction curves of the growing noise wave with the main magnetic field as parameter.

3.8 BEAM NOISE MEASUREMENTS ON A MEDIUM PERVEANCE GUN

Some measurements were made on a gun developed by the Bell Telephone Laboratories. This gun had a convergence half angle of 13°, a perveance of 0.45×10^{-6} amp/volt$^{3/2}$, and produced a beam about 0.08 inch in diameter. The heater construction was such as to produce an observable magnetic field at the cathode surface (a few gauss). As with the previous convergent gun, a strong growing noise wave was observed superimposed upon the standing-wave pattern. The growing part of the noise wave, however, fluctuated violently at 60 cps when viewed on an oscilloscope. This was soon traced to the heater. It was observed that the growing noise might vary by approximately 10 db, depending upon the polarity of the heater current, and that this bore a definite relation to the direction of the main focusing field; reversing one required reversing the other to produce a given effect. Previous measurements had indicated that the main focusing field of several hundred gauss produced a leakage field of a few gauss at the cathode, outside the main magnetic field. Again, with the aid of an auxiliary solenoid around the gun, it was possible to produce fields of a few gauss at the cathode. With a proper auxiliary field (a few gauss) the growing noise wave could be completely eliminated.

3.9 BEAM INSTABILITY

In the portion of the beam with growing noise wave present, it was observed that the beam itself became highly unstable. This was determined by observing the fluctuations in the collector current when a movable vane was arranged to partially intercept the beam. When this was done in a region of normal noise (the gun end of the drift tube), nothing special was noted on the oscilloscope except a reduction in current. When the same experiment was performed in the growing-noise region, one observed on the 10 Mc/sec wide oscilloscope an apparent "white" noise whose amplitude was almost half the dc value.

The growing noise wave itself was considerably reduced if a small portion of the beam was intercepted by a movable vane in front of the cavity. For the same amount of interception current, greater noise reduction could be achieved with knife-edge interception than with a circular aperture in the vane. Typical results obtained with the

Table I. Noise Level at a Fixed Cavity Position with and without Interception

Interception (per cent)	Noise With		
	No Interception (db above shot noise)	Knife-Edge Interception (db above shot noise)	Circular Aperture Interception (db above shot noise)
0	28	—	—
5	—	21	23.5
20	—	15	18.5

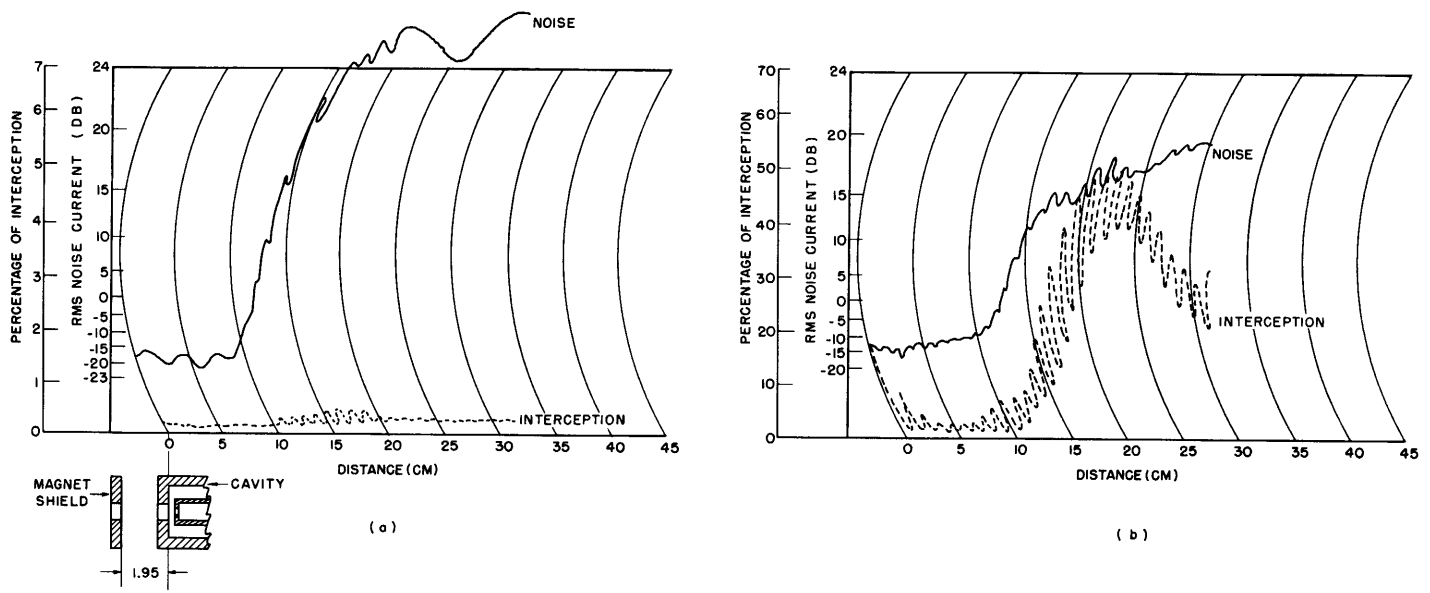

Fig. 19. RMS noise current versus cavity position for steady-flow, medium-perveance, convergent electron beam. V_o = 1000 volts; $I_{cathode}$ = 14.4 ma; H = 600 gauss; pressure $\approx 5 \times 10^{-7}$ mm Hg.

medium-perveance gun described in section 3.8 are given in Table I and in Fig. 19. Table I shows the noise level above pure shot noise at a fixed cavity position with and without interception. Figure 19(a, b) gives typical noise versus distance characteristics and their associated interception curves without any interception by the vane and with interception by a circular aperture in the vane, respectively. The noise-reducing effect of the interception is evident from these curves. It is also very noteworthy that the steeply rising portion of the growing noise wave coincides with a violently scalloping region of the electron beam.

IV. MEASUREMENTS ON CONFINED-FLOW ELECTRON BEAMS

4.1 INTRODUCTION

Confined-flow beams are produced by electron guns which are immersed in the magnetic field. The paths of the electrons are different from those of a convergent-flow beam. Though detailed analyses are available elsewhere (1, 6), a brief summary seems appropriate at this point.

Section III presented the conditions for Brillouin-flow. In an ideal Brillouin-flow, the gun is shielded from the magnetic field. After entering the field, all electrons encircle the axis of the beam as they spiral along the drift tube. The radial distance between any individual electron and the axis should remain constant theoretically. If the Brillouin-flow is perturbed, this radial displacement varies periodically as the electrons drift toward the collector. The periodicity should correspond to $(2)^{1/2}$ times the cyclotron wavelength. If the beam is fully neutralized, Brillouin-flow cannot occur. In a neutralized beam, every electron has to cross the axis instead of encircling it. The resulting periodicity now becomes equal to the cyclotron wavelength. The actual measurements – as described in Section III – indicated a perturbed flow somewhere in between the two theoretical cases just mentioned.

In contrast to its location in the convergent-flow beam, in the confined-flow beam the cathode is located in the magnetic field. Thus the electrons, if launched correctly and with no radial space-charge forces, would travel in straight, parallel paths. With negative space charge in the beam, the electrons would start spiraling again. The helical paths of the electrons do not encircle or cross the axis of the beam as they do in convergent flow. With increasing magnetic fields, each electron is forced to travel closer to the center of its own helical path. At the same time, the angular velocity of the electrons also decreases. Thus, increasing magnetic fields tend to straighten out the paths of the electrons.

With a fully neutralized space charge, a perfectly parallel beam would be possible if initial conditions are correct. If they are not, because of imperfect focusing or transverse thermal velocities, for instance, a perturbed beam will result. The perturbation wavelength should again correspond to the cyclotron wavelength.

This section gives a detailed description of the noise measurements on confined-flow electron beams. These measurements were performed under both steady-flow and pulsed operations. Experiments were also made to determine the effect of interception current on the beam noise.

The confined-flow beams were produced by a parallel gun with the following parameters:

Perveance	0.05×10^{-6}	amp/volt$^{3/2}$
Cathode diameter	0.040	inch

Unless specifically stated otherwise, these gun characteristics should be assumed for all measurements in this section.

All measurements were first performed with oxide-coated cathodes. Some of them were repeated thereafter with an impregnated Philips cathode. One paragraph of this section compares the results obtained with Philips cathodes with the measurements on oxide-coated ones.

4.2 NOISE MEASUREMENTS ON STEADY-FLOW BEAMS

A number of noise-current measurements were made on steady-flow beams for various values of the magnetic field, beam-forming electrode bias, and cathode temperature. In all measurements, the interception did not exceed 0.1 per cent of the collector current. An accelerating voltage of 1500 volts was applied between the cathode and the anode.

The first set of measurements investigated the effect of the magnetic field on the noise along the beam. It was found that above a required minimum collimating field, the strength of the magnetic field had no effect on the noise. During these measurements, the field was varied from 172 gauss to 602 gauss. A large number of noise-current curves were recorded for different values of the magnetic field. A typical curve of the rms noise current is shown in Fig. 20 for a magnetic field of 301 gauss. In all of these curves, a standing-wave ratio of approximately 14 db to 15 db was observed. The first minimum was approximately 26 db to 27 db below shot-noise level. The next minimum was even deeper. The depth of the second minimum reached 29 db to 31 db below the full shot-noise level of the beam. All curves could be reproduced.

Next, the effect of biasing voltage was investigated. This was done by appling -6, -3, -1.5, 0, 1.5, 3, and 6 volts between the cathode and the beam-forming electrode. The corresponding collector currents were 2.1, 2.4, 2.6, 2.8, 2.9, 3.1, and 3.4 ma, respectively. A collimating field of 301 gauss and a beam voltage of 1500 volts were used. The resulting noise-current curves showed no essential change from that of Fig. 20, in spite of the variations of the biasing voltage and the collector current.

The next experiments were concerned with the effect of cathode temperature on the beam noise. Of course, the cathode temperature could only be varied in a limited range. The cathode had to be hot enough to sustain space-charge-limited emission. The

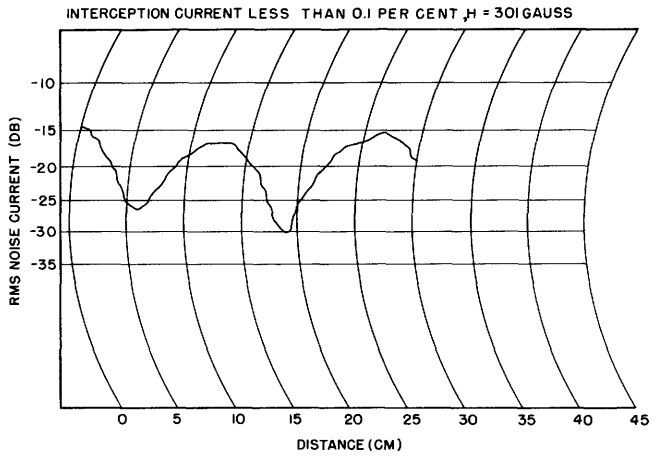

Fig. 20. RMS noise current versus cavity position for confined, steady-flow electron beam. V_o = 1500 volts; I_o = 2.8 ma; pressure $\approx 1.5 \times 10^{-7}$ mm Hg.

evaporation of nickel determined the upper temperature limit. It was observed that as the cathode temperature varied, the perveance changed slightly. But as far as the noise characteristics were concerned, no appreciable change was noticed in an approximately 200°C range which was explored in the vicinity of the normal operating temperature. The noise-current curves were again strikingly similar to the one shown in Fig. 20.

A few additional remarks are appropriate before concluding the discussion of steady-flow measurements. First, there were more than a dozen noise-current curves with second minima which were 30 db below shot-noise level. According to the prevailing theory of partition noise (8), 0.1 per cent interception current alone could introduce that amount of noise. Since the interception currents encountered during the measurements were of that order of magnitude, the question arose whether or not the 30-db limit was determined by the partition noise or by the finite noise standing wave. Section VI will include a few experiments that shed more light on this problem.

It must also be mentioned that throughout the steady-flow measurements, the current density drawn from the cathode exceeded 350 ma/cm^2. Current densities of that magnitude were usually considered too high for low noise application of oxide-coated cathodes.

In concluding the discussion of the steady-flow measurements, it must be emphasized that for the particular parameters of these measurements no growing noise waves were observed under steady-flow operation. Under very special operating conditions, however, growing noise waves could be excited on a confined, steady-flow electron beam.

4.3 NOISE MEASUREMENTS ON UNNEUTRALIZED CONFINED-FLOW BEAMS

As in the convergent-flow experiments, the noise measurements on confined-flow beams were repeated under pulsed operation. To avoid neutralization, a pulse duration of 0.7 μsec was used at a 4000-cps repetition rate. As mentioned previously, the

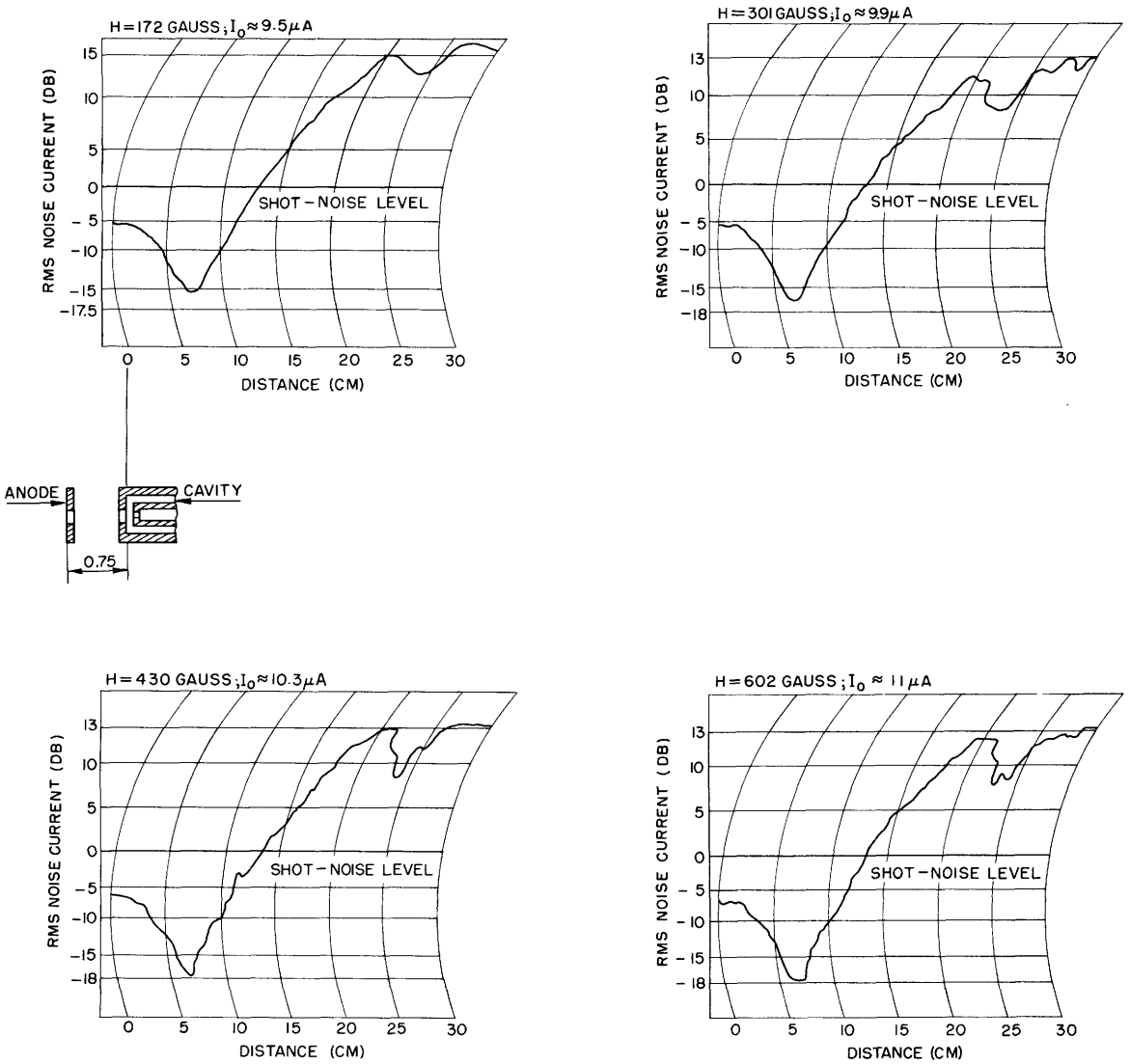

Fig. 21. RMS noise current versus cavity position for space-charge-limited, confined-flow, pulsed electron beam. V_o = 1500 volts; pressure $\approx 4 \times 10^{-7}$ mm Hg.

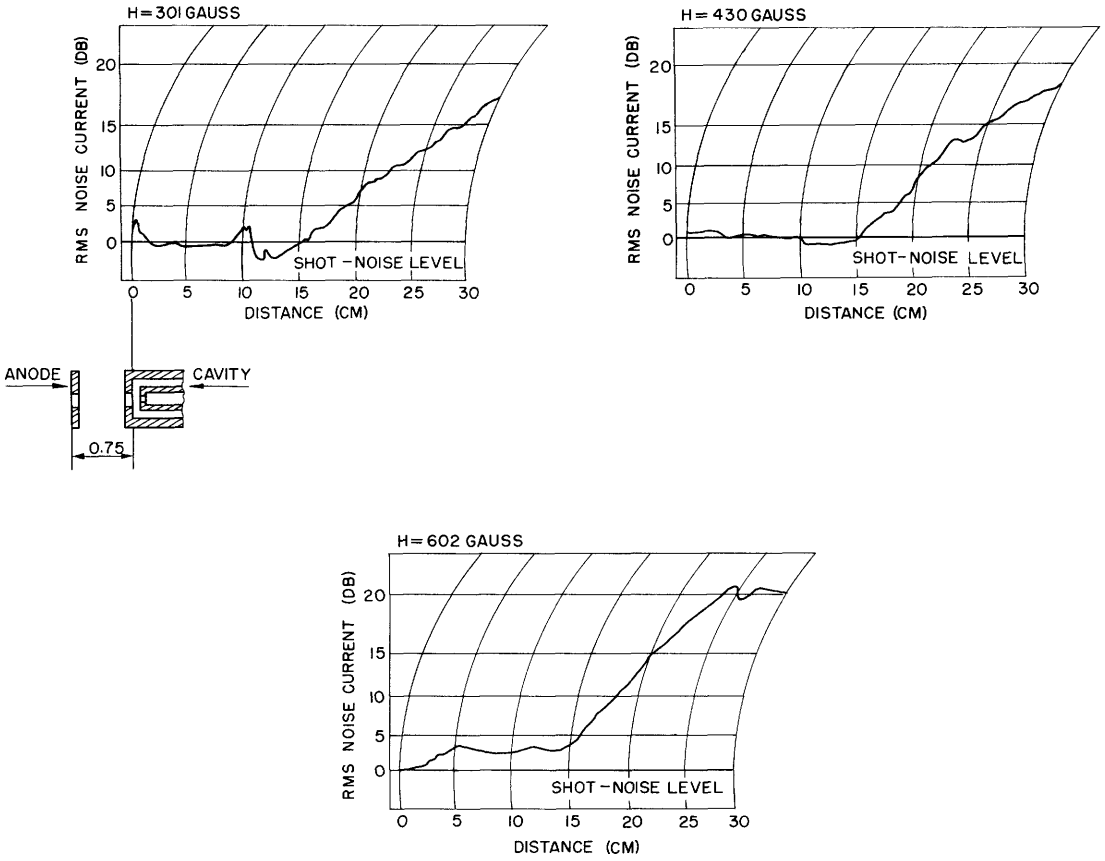

Fig. 22. RMS noise current versus cavity position for temperature-limited, confined-flow, pulsed electron beam. V_o = 1500 volts; $I_o \approx 0.9$ μa; pressure $\approx 4 \times 10^{-7}$ mm Hg.

generated pulse had a very short rise time and no observable overshoot.

Figure 21 shows a set of noise-current curves obtained with a 1500-volt pulse amplitude. The magnetic-field strength was the varying parameter for the curves of Fig. 21. It was evident from Fig. 21 that the magnetic field did not appreciably affect the noise characteristics. A similar observation was made for the steady-flow measurements. But differing from the steady-flow operation, a large growing noise wave was always excited whenever the beam was operated with the 0.7-μsec voltage pulse. The growing wave started after a relatively deep first minimum. It rose rapidly to approximately 13 db above the shot-noise level and then leveled off.

The noise measurements discussed so far were all performed on space-charge-limited electron beams. The measurements were repeated after the cathode temperature was lowered to produce a temperature-limited electron beam. Figure 22 shows the noise-current measurements for the temperature-limited case. The magnetic field was again the varying parameter and 1500 volts the pulse amplitude.

Figure 22 indicates the existence of growing noise wave even in temperature-limited electron beams under certain conditions. The growing noise seemed somewhat stronger than under space-charge-limited conditions. With the exception of one curve, no sign of saturation was noticeable. However, during the recording of that particular curve, the collector current dropped suddenly to 0.5 μa. It would be difficult to tell whether the break in the growing noise curve was caused by the current decrease or a saturation phenomenon.

4.4 NOISE MEASUREMENTS ON BEAMS WITH VARIABLE NEUTRALIZATION

The steady-flow measurements on confined-flow beams showed finite standing waves of noise along the beam. In general, no growing waves were superimposed upon this standing wave. With a 0.7-μsec pulse, however, there was a strong growing wave excited all the time. Attempts have been made to bridge the steady-flow noise measurements and the ones performed under pulsed operation. Similar experiments have been already described in section 3.5 in connection with the convergent-flow beam measurements. Pulsing the beam with a very long voltage pulse produced a beam that was unneutralized at the beginning, but reached its final degree of neutralization toward the end of the pulse. By applying a gate of relatively short duration to the noise output with various time delays after the leading edge of the pulse, it was possible to make sets of intermediate measurements between unneutralized and neutralized conditions. The apparatus used to perform this experiment was illustrated before in Fig. 7. The pulse modulator maintained a 50 per cent duty cycle with a variable repetition rate and voltage. The pulses were flat and had a rise time of approximately 1.5 μsec to 2.5 μsec.

The modulator pulse duration was first adjusted to 2500 μsec. An approximately 1.5-μsec gating pulse was applied with time delays varying from 0 μsec to 1000 μsec. The delay was again measured from the time when the final pulse amplitude was reached. Thus zero time delay was really approximately 2.5 μsec after the beam started. The

resulting noise curves were again similar to the one shown in Fig. 20. No growing noise wave was observed for any time delay of the gating pulse. The standing wave was unaffected by time delay (between 2.5 μsec to 1000 μsec), magnetic field, and cathode temperature. The magnetic fields varied from 172 gauss to 602 gauss. The effect of cathode temperature was explored in an approximately 200°C range about the normal operating temperature. Changing the pulse length did not produce any growing noise wave either. Pulse durations of 25, 250, 2500, and 25,000 μsec were tried. The pulse amplitude was 1500 volts in all cases. Under these particular conditions, no growing-noise waves were observed. The strange oscillation-like phenomena shown in Fig. 17, which were observed for a convergent-flow beam under similar conditions, were absent in these measurements.

When the fixed, 0.7-μsec pulser was reconnected, however, growing noise waves were again observed. The only apparent difference was the fact that the fixed, 0.7-μsec pulse had a very short rise time whereas the rise time of the variable-width pulse was approximately 1.5 μsec to 2.0 μsec.

4.5 NOISE MEASUREMENTS WITH A PHILIPS CATHODE IN THE CONFINED-FLOW GUN

Almost all the measurements discussed so far in this section were repeated with a Philips cathode in the parallel gun. The diameter of the emitting impregnated tungsten pellet was 0.040 inch. The oxide-coated button had the same diameter. However, the tungsten pellet was press-fitted into a cylindrical molybdenum receptacle. The wall thickness of this receptacle was 0.006 inch near the emitting surface. Because of the increased over-all cathode diameter, the beam-forming electrode aperture had to be opened up somewhat. The resulting perveance became considerably larger than for the gun with oxide-coated cathodes. The cathode could not maintain good space-charge-limited emission under steady-flow operation whenever the current-density requirements approached 0.5 amp/cm^2. Experimental evidence showed that ion bombardment was the main source of trouble.

A number of noise measurements were made in spite of the fact that the emission seemed to be slightly temperature limited. The results agreed in general with the measurements with oxide-coated cathodes. The steady-flow and the long, variable-pulse measurements resulted in standing waves. The standing-wave ratio was approximately 12 db to 13 db. The maxima were about 14 db to 15 db below the pure shot-noise level of the beam. The magnetic field strength did not affect the noise characteristics appreciably. No growing wave was observed under steady-flow or long-pulse operating conditions. However, as soon as the fixed 0.7-μsec pulser modulated the beam, an exceedingly violent growing noise wave was excited.

V. STEADY-FLOW MEASUREMENTS ON A LOW-NOISE, THREE-REGION GUN

5.1 INTRODUCTION

The generally accepted expression for the noise figure of a traveling-wave tube is given by (20, 9)

$$F = 1 + \frac{1}{2}(4-\pi)\frac{T_c}{T}\frac{r}{C} f(QC,\ d,\ \delta z)$$

where T_c is the cathode temperature in °K; T is the room temperature in °K; C is Pierce's gain parameter (22); $r = \overline{v_m^2}/\overline{v_a^2}$ is the noise-reduction factor; v_m is the amplitude of maximum velocity fluctuation in the beam; v_a is the amplitude of initial fluctuation at the cathode; and, $f(QC,\ d,\ \delta z)$ is the function defined and calculated by Watkins (9). From this expression, it becomes evident that the noise figure of the traveling-wave tube can be improved if means are found to decrease the noise-reduction factor r, before the beam enters the helix. Watkins (9) obtained a reduction of r with accelerating and decelerating gaps separated by constant potential drift tubes. By means of this velocity-jump method, he designed and built traveling-wave tube amplifiers which had gains of 10 db to 20 db and noise figures of 10 db to 12 db.

R. W. Peter (20) achieved the same goal with what he called a "three-region gun." Peter showed that "not only is the three-region gun more flexible as regards control of electrical drift angle, but that in addition, the theory indicates that a somewhat greater noise reduction can be expected from it." The noise figure Peter obtained was of the order of 8 db with a gain of 15 db.

Traveling-wave tubes have been built at the Bell Telephone Laboratories with noise figures of the order of 7 db. The construction of these tubes is similar to the three-region tube of Peter, but they have higher operating frequencies and currents. Since the theories and the experimental results of traveling-wave tubes with velocity jumps or multiple-region guns are available elsewhere (9, 20), further discussion would be repetitious. Instead, a number of noise-current measurements are presented in the next paragraph. These measurements were performed on one of Peter's three-region guns. The theoretical study of Peter indicated the following design considerations. The first anode should be at as low a potential as possible; therefore, it should be located as close to the cathode as is practicable in order to achieve maximum perveance. The second anode should be spaced from 1 to 1.7 times the first anode-cathode distance away from the first anode. The third anode should be at the helix potential and close to the second anode. Empirical results, however, showed that the spacing between the second and third anodes should be approximately the same as between the first and second anodes. This spacing had to be approximately twice the distance between the first anode and the cathode.

The cathode protruded into the space between the beam-forming electrode and the first anode. By varying the cathode-electrode potential, the perveance and the initial divergence of the gun could be continuously changed.

5.2 NOISE MEASUREMENTS ON A THREE-REGION GUN

All measurements were performed under steady-flow conditions. The measuring apparatus was described before and is illustrated in Fig. 5. The three-region gun used in these measurements was very obligingly put at the writer's disposal by Dr. Peter. The specifications supplied with the gun indicated the following operating conditions:

Cathode temperature	1050-1100°C
Cathode current	300 μa
Beam-forming-electrode voltage	0 volts
First-anode voltage	37 volts
Second-anode voltage	110 volts
Third-anode voltage	530 volts
Magnetic field	455 gauss

It was found, however, that with the voltages given above the beam current was about 25 per cent more. No current was intercepted by any of the electrodes.

Figure 23 shows a number of noise-current curves as functions of distance along the drift tube. In all of these curves the cathode temperature, the beam-forming-electrode voltage, and the first-anode voltage were adjusted for the prescribed values. For one curve, the second- and third-anode voltages have also the recommended magnitude. For the other curves, however, either the second- or the third-anode voltage differed from the recommended data. The essential characteristics of the noise-current curves may be summarized as follows. The noise-current maxima were at least 19 db below the pure shot-noise level, provided the second- or third-anode voltage was not grossly misadjusted. Under the same conditions, the standing-wave ratio did not exceed 7 db. By suitably adjusting the second-anode voltage, the standing-wave ratio could be reduced to approximately 1.5 db. The indications were that with a few more trials even further reduction could have been obtained. Under most conditions, the product $I_{max} I_{min}$ remained remarkably constant at 22 ± 1 db. (I_{max} and I_{min} denote the rms noise-current maximum and minimum, respectively.) Exceptions occurred when the second and third anodes, or the second anode and the cathode, were tied together; the resulting product of $I_{max} I_{min}$ then became 19 ± 0.5 db and 17 ± 0.5 db, respectively. In both cases, however, the collector current changed by approximately 15 per cent.

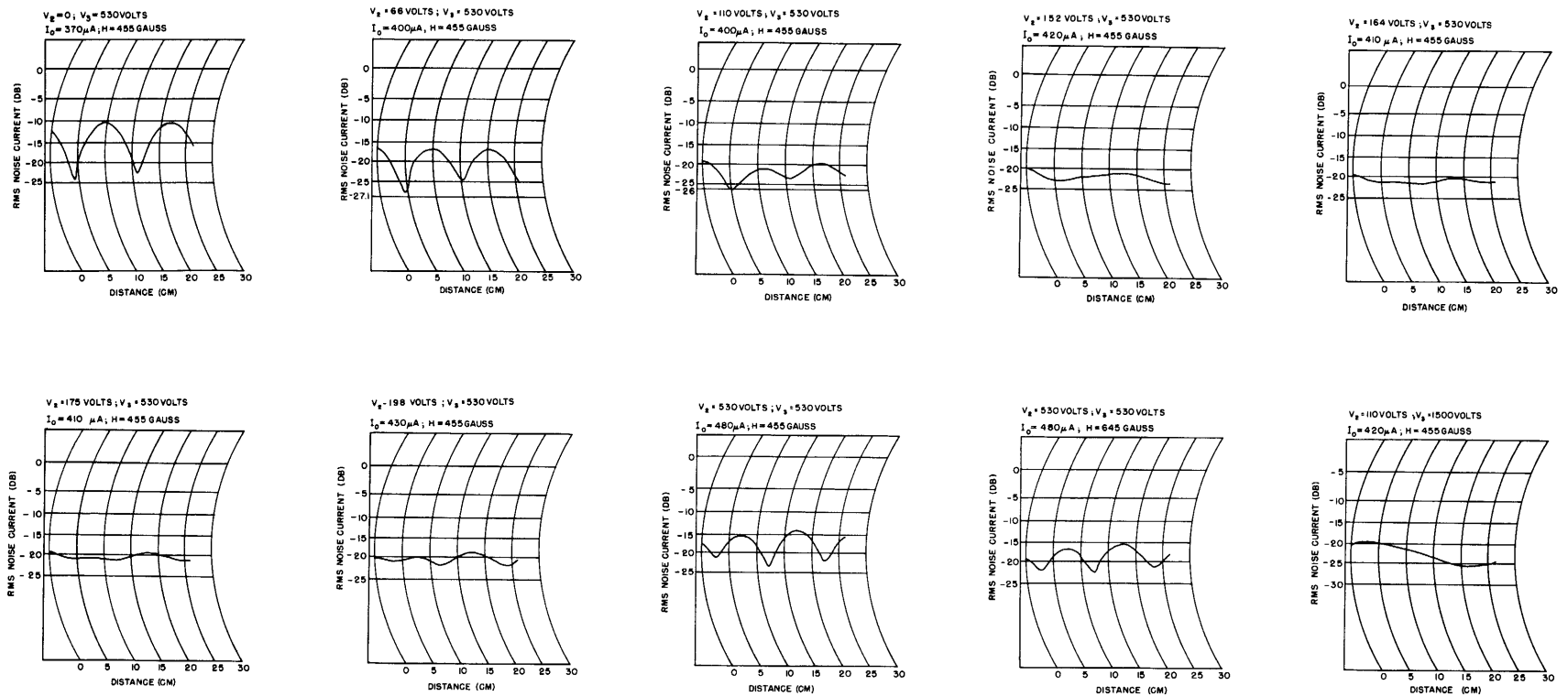

Fig. 23. RMS noise current versus cavity position for the low-noise, three-region gun. V_1 = 37 volts; pressure $\approx 9 \times 10^{-8}$ mm Hg.

VI. NOISE MEASUREMENTS CONCERNING THE EFFECT OF INTERCEPTION CURRENT

6.1 INTRODUCTION

In connection with the deep noise-current minima of Section IV, the following question has to be answered. Were those minima the result of the finite noise standing wave, or did the partition noise limit the measurements? The prevailing explanation and treatment of partition noise are due to North (8). According to North, the fluctuation $\overline{i_n^2}$ present in the current I_n which is collected by the nth collector is represented by

$$\overline{i_n^2} = \left[1 - \frac{I_n}{I_c}(1 - \Gamma^2)\right] (I_n \cdot 2e\Delta f) \tag{1}$$

where I_n is the dc current collected by the nth electrode, $\overline{i_n^2}$ is the mean-square noise current in the dc current flowing to the nth electrode, I_c is the cathode current, Γ^2 is the space-charge-smoothing factor, e is the electronic charge, and Δf is the bandwidth. For complete space-charge smoothing ($\Gamma^2 \to 0$), Eq. 1 becomes approximately

$$\overline{i_n^2} \approx \frac{I_c - I_n}{I_c} 2eI_n\Delta f \tag{2}$$

The factor $(I_c - I_n)/I_c$ represents actually the fraction of the cathode current which does not reach the nth collector. In a traveling-wave tube, I_n would represent the collector current and $(I_c - I_n)/I_c$ the interception current. If, in a traveling-wave tube, the interception occurs before the beam enters the circuit, the beam current passing through the

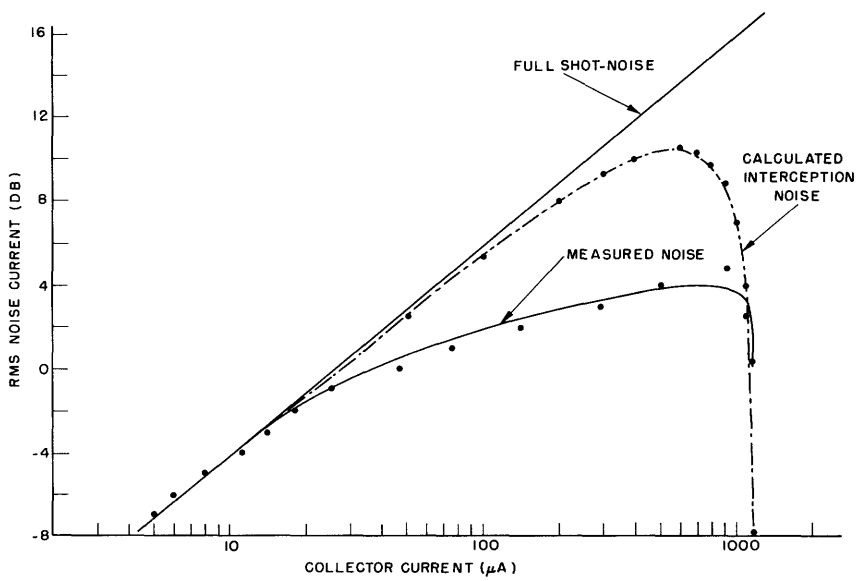

Fig. 24. Muehe's interception noise measurement.

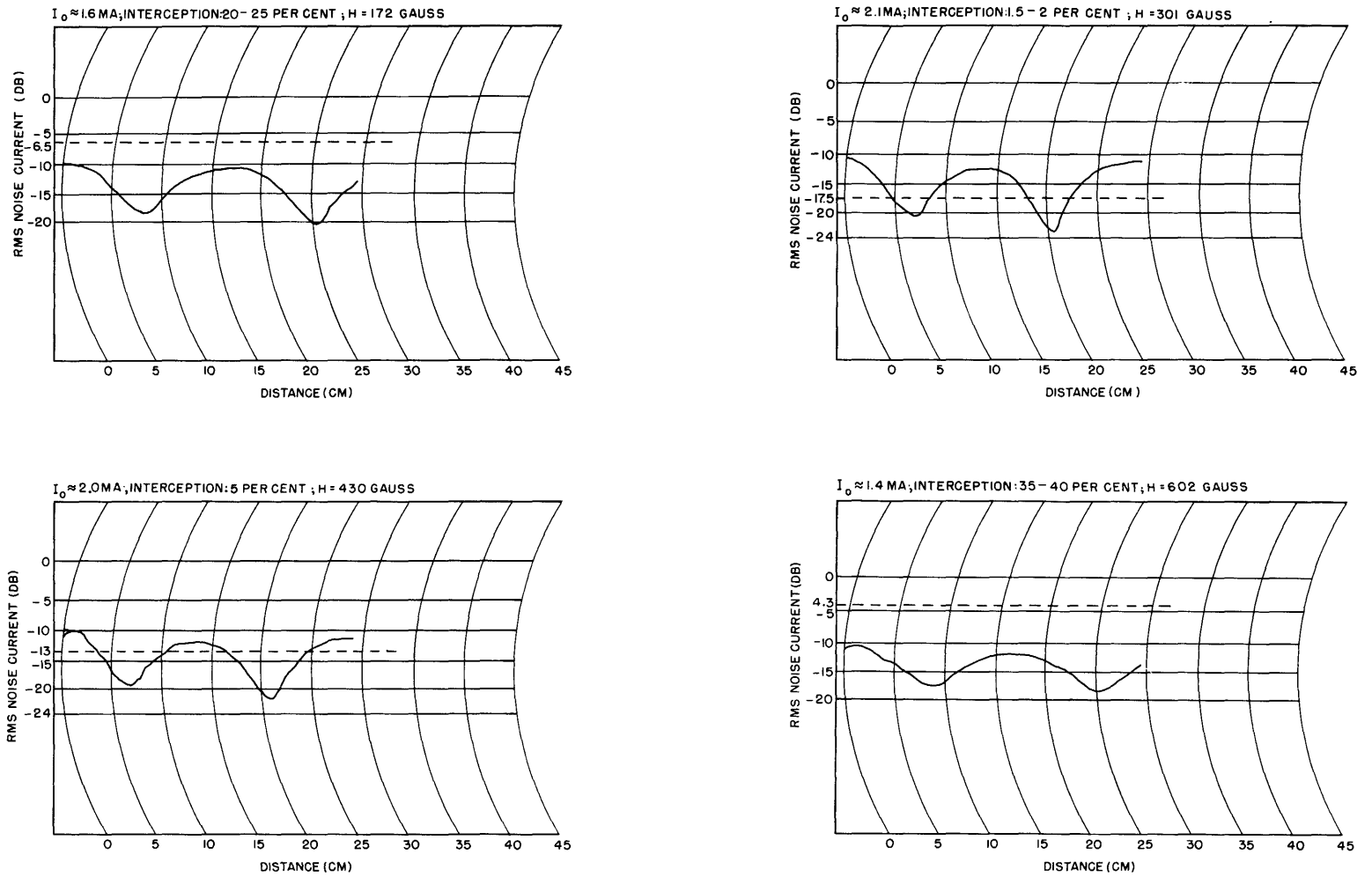

Fig. 25. RMS noise current versus cavity position of a confined-flow beam with large interception current. V_o = 1500 volts; pressure $\approx 2 \times 10^{-7}$ mm Hg.

circuit contains an additional noise current. This noise current is uncorrelated with the noise velocities and currents contained otherwise by the beam. In the past (9), it was generally assumed that Eq. 2 gives the magnitude of this noise current. C. E. Muehe verified Eq. 2 experimentally to a certain degree. He intercepted almost all of the cathode current with a movable shutter so that only a small fraction could reach the collector. If the collector current was small, then it contained full shot noise. The experiments to be described in this section, however, indicate that Eq. 2 does not hold if the collector current is not small compared to the interception current. Muehe's original data sheet revealed that he obtained full shot noise only when the collector current was less than approximately 2 per cent of the cathode current. It becomes evident from Fig. 24 that for collector currents of more than 2 per cent of the cathode current, Muehe's data (24) show considerably less beam noise than would be expected from Eq. 2. Thus, it can be stated that Muehe's partition noise measurements did not disagree with the experimental results of the next paragraph.

6.2 THE EFFECT OF INTERCEPTION CURRENT ON THE NOISE IN CONFINED-FLOW BEAMS

The parallel gun used in the following measurements was identical to the one described in Section IV. A portion of the beam was intercepted by an aperture plate. This aperture plate was attached to the anode on the side, away from the cathode. Figure 25 shows how the interception current affected the noise measurements. Even though the noise-current minima were raised as a result of interception current, the noise current was usually much below the level that would be predicted by Eq. 2. The noise level as computed from Eq. 2 is indicated in each curve by a dashed line.

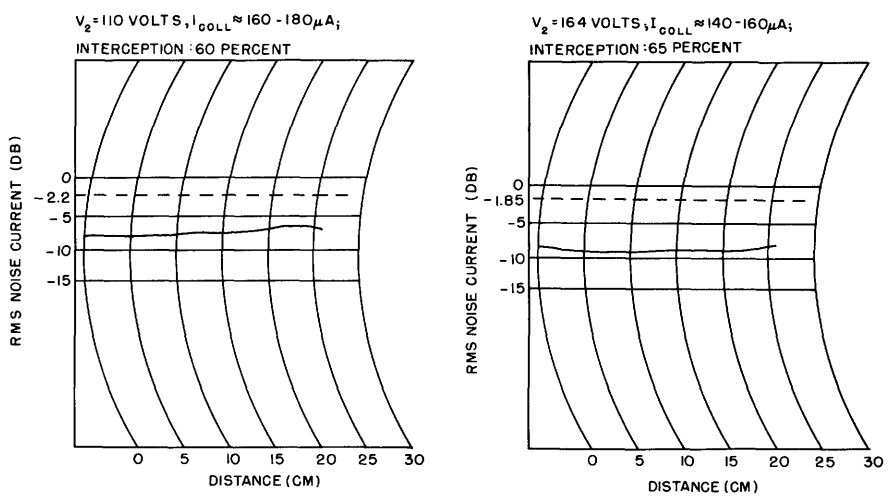

Fig. 26. RMS noise current versus cavity position using the three-region gun with large interception current. V_1 = 37 volts; V_3 = 530 volts; H = 455 gauss; pressure $\approx 8.5 \times 10^{-8}$ mm Hg.

6.3 THE EFFECT OF INTERCEPTION CURRENT ON A LOW-NOISE BEAM

Peter's low-noise, three-region gun was used to produce a low-noise beam. Section V described the noise measurements obtained without interception current. Figure 26 shows how the noise characteristics were affected when 60-65 per cent of the beam was intercepted. The interception was done this time with the aid of an aperture in the shutter attached to the moving cavity. The curves of Fig. 26 were taken with anode voltage corresponding to (a) the values recommended by Peter for minimum noise figure; (b) the values at which the noise-standing-wave pattern was smoothed out. Figure 26 also shows that the noise remained much below the level computed from Eq. 2. The noise level calculated from Eq. 2 is again indicated by dashed lines.

VII. CONCLUSION

A few words should be said about the accuracy of the measurements presented in the previous sections. The noise-current curves were reproducible within one decibel. However, a considerable amount of inherent instability was noticeable in the growing noise waves for levels greater than 10 db above full shot noise. The noise-current curves illustrated in this report are only typical samples of a much larger number of noise measurements that were recorded during the course of the experiments. The results of these experiments may be summarized as follows.

The noise-current standing-wave ratio along the beam is finite. The greatest standing-wave ratio observed was about 15 db to 16 db. It is extremely doubtful that the observed minima were limited by partition noise.

Partition-current noise, produced by intercepting an annulus of a circular beam, was considerably less than that predicted by North's (8) analysis for interception by a fine grid.

The variation of noise along a "Brillouin-focused" beam may exhibit two main characteristics:

(a) A regular standing wave with the period equal to the reduced plasma wavelength.

(b) Rapid increase of noise with distance in the latter portion of the beam, the level sometimes exceeding shot noise by more than 30 db. This has been called the "growing noise wave."

The growing noise waves could be reduced or eliminated by a considerable increase in the main focusing magnetic-field strength, relatively weak auxiliary magnetic field in the gun region, and increased ion neutralization of the beam. The growing noise wave is very closely associated with a violent instability of the beam itself and the type and quality of the cathode proper. While there are a number of known mechanisms which can support growing waves in an electron beam, none of the suggested ones could be reconciled, so far, with all the experimental results. Further experiments concerning the possibility of signal amplification seem to be in order. Also, the velocity distribution of electrons at the cathode should be re-examined carefully in the light of recent

experiments on oxide-coated cathodes (25, 26). It is the author's belief that radial fluctuations in the beam play an important rôle in the mechanism of the observed growing noise waves.

Noise measurements on simple, one-region, confined-flow guns generally resulted in a standing-wave pattern of noise. Growing noise waves were excited whenever the beam was pulsed with a short pulse having a sharp rise time. Above a required minimum collimating field, the strength of the magnetic field had no appreciable effect on the noise. During these measurements the field varied from 172 gauss to 602 gauss.

Peter's low-noise, three-region gun was tested only under steady-flow conditions. It was shown how the standing-wave pattern could be varied with adjustment of the voltage on the second anode. It was apparent that over a wide range the product $I_{max} I_{min}$ remained substantially constant, and that the transformer in the anode regions is capable of matching the noise-standing-wave ratio to unity. This result confirms a recent, somewhat restricted, theory of Pierce (27) and a more general one of Haus (28). They proved that the product $K_d I_{max} I_{min}$ must be conserved as long as no rf power is added or subtracted from the beam. K_d is the impedance of the beam, and I_{max} and I_{min} denote the rms noise-current maximum and minimum, respectively. According to the calculations of Pierce (7)

$$\frac{I_{max} I_{min}}{2eI_o \Delta f} = 0.822 \frac{\omega K T_c}{2\omega_q e V_o}$$

For the parameters appropriate to this gun, we should have a value of $I_{max} I_{min}$ = 23 db below shot noise, as compared with an observed level of 22 db below shot noise.

Acknowledgment

The author wishes to express his sincere gratitude to Professor L. D. Smullin for his invaluable guidance and advice; and to Professor L. J. Chu, Professor H. A. Haus, Mr. D. L. Bobroff and Mr. H. Shelton for many valuable discussions and suggestions. The author is also indebted to Dr. R. W. Peter and many researchers of Bell Laboratories for their continued interest and help in his work.

Bibliography

1. C. E. Muehe, Noise figure of traveling-wave tubes, Technical Report 240, Research Laboratory of Electronics, M.I.T. (1952).
2. Research Laboratory of Electronics, Drawings, Series 1248.
3. D. Alpert, New developments in the production and measurement of ultra high vacuum, J. Appl. Phys. 24, 860-876 (1953).

4. K. Spangenberg, L. M. Field, and R. Helm, The production and control of electron beams (Federal Telephone and Radio Corporation, Newark, N. J., 1942, limited edition).

5. R. H. Dicke, The measurement of thermal radiation at microwave frequencies, M.I.T. Radiation Laboratory Report No. 787, Aug. 22, 1945.

6. J. R. Pierce, Theory and Design of Electron Beams (D. Van Nostrand Co., Inc., New York, 1949).

7. C. Fried, Research Laboratory of Electronics Computation Book No. 738.

8. B. J. Thompson, D. O. North, and W. A. Harris, Fluctuations in space-charge-limited currents at moderately high frequencies, RCA Rev. 4, No. 3, pp. 269-285 (Jan. 1940).

9. D. A. Watkins, Noise reduction in beam type amplifiers, Technical Report 31, Electronics Research Laboratory, Stanford University, March 15, 1951.

10. C. C. Cutler and C. F. Quate, Experimental verification of space charge and transit time reduction of noise in electron beams, Phys. Rev. 80, 875-8 (1950).

11. W. C. Hahn, Small signal theory of velocity-modulated electron beams, General Electric Rev. 42, 258-70 (1939).

12. S. Ramo, Space charge and field waves in an electron beam, Phys. Rev. 56, 276-83 (1939).

13. L. Brillouin, A theorem of Larmor and its importance for electrons in magnetic fields, Phys. Rev. 67, 260-266 (1945).

14. C. R. Moster and J. P. Molnar, Some calculations of the magnetic field requirements for obtaining Brillouin flow in cylindrical electron beams, MM-51-2940-1, MM-51-2960-1 Bell Telephone Laboratories, Jan. 16, 1951.

15. A. J. Rack, Effect of space charge and transit time on the shot noise in diodes, Bell System Tech. J. 17, 592 (1938).

16. F. B. Llewellyn, Electron-Inertia Effects (Cambridge University Press, London, 1943).

17. F. B. Llewellyn and L. C. Peterson, Vacuum-tube networks, Proc. IRE 32, 136-66 (1944).

18. L. T. Zitelli, Space charge effects in modulated electron beams, Ph. D. Thesis, Department of Electrical Engineering, Stanford University (1950).

19. H. E. Rowe, Shot noise in electron beams at microwave frequencies, Sc. D. Thesis, Department of Electrical Engineering, M.I.T. (1952).

20. R. W. Peter, Low-noise traveling-wave amplifier, RCA Rev. 13, 344-368 (1952).

21. B. H. Wadia, The influence of positive ions on electron-beam profiles, Technical Report 74, Electronics Research Laboratory, Stanford University, Jan. 28, 1954.

22. J. R. Pierce, Traveling-Wave Tubes (D. Van Nostrand Co., Inc., New York, 1950).

23. R. W. Peter, Research and development on microwave generators, mixing devices and amplifiers, RCA Quarterly Reports 1 to 4, May 1951 to April 1952.

24. C. E. Muehe, Research Laboratory of Electronics Computation Book No. 700.

25. R. Loosjes and C. G. J. Jansen, The velocity distribution of electrons of thermionic emitters under pulsed operation, Part I, Philips Res. Rep. 8, 21 (1953).

26. R. Loosjes, H. J. Vink, and C. G. J. Jansen, Thermionic emitters under pulsed operation, Philips Tech. Rev. 13, 337 (1952).

27. J. R. Pierce, A theorem concerning noise in electron streams, J. Appl. Phys. 25, 931 (1954).

28. H. A. Haus, Noise and signal propagation along electron beams at microwave frequencies, Ph. D. Thesis, Department of Electrical Engineering, M.I.T. (1954).